

Z boson production in $p + \text{Pb}$ collisions at $\sqrt{s_{NN}} = 5.02$ TeV measured with the ATLAS detector

G. Aad *et al.*^{*}
 (ATLAS Collaboration)

(Received 23 July 2015; revised manuscript received 23 September 2015; published 30 October 2015)

The ATLAS Collaboration measures the inclusive production of Z bosons via their decays into electron and muon pairs in $p + \text{Pb}$ collisions at $\sqrt{s_{NN}} = 5.02$ TeV at the Large Hadron Collider. The measurements are made using data corresponding to integrated luminosities of 29.4 and 28.1 nb^{-1} for $Z \rightarrow ee$ and $Z \rightarrow \mu\mu$, respectively. The results from the two channels are consistent and combined to obtain a cross section times the $Z \rightarrow \ell\ell$ branching ratio, integrated over the rapidity region $|y_Z^*| < 3.5$, of 139.8 ± 4.8 (statistical) ± 6.2 (systematic) ± 3.8 (luminosity) nb. Differential cross sections are presented as functions of the Z boson rapidity and transverse momentum and compared with models based on parton distributions both with and without nuclear corrections. The centrality dependence of Z boson production in $p + \text{Pb}$ collisions is measured and analyzed within the framework of a standard Glauber model and the model's extension for fluctuations of the underlying nucleon-nucleon scattering cross section.

DOI: [10.1103/PhysRevC.92.044915](https://doi.org/10.1103/PhysRevC.92.044915)

PACS number(s): 25.75.Bh, 25.75.Dw, 14.70.Hp

I. INTRODUCTION

The study of electroweak bosons in $\text{Pb} + \text{Pb}$ collisions at the Large Hadron Collider (LHC) at CERN has demonstrated that the production rate of non-strongly interacting particles scales with the number of nucleon-nucleon collisions, $\langle N_{\text{coll}} \rangle$. This has been observed for photons [1], W bosons [2,3], and Z bosons [4,5]. The momentum and rapidity distributions of Z boson yields are consistent with PYTHIA [6] simulations of pp collisions multiplied by the average nuclear thickness function, $\langle T_{\text{AA}} \rangle$, which is equivalent to $\langle N_{\text{coll}} \rangle$ divided by the total nucleon-nucleon cross section [4]. Z boson production in $\text{Pb} + \text{Pb}$ collisions was found to be consistent with next-to-leading-order perturbative quantum chromodynamics (NLO QCD) calculations that disregard nuclear modifications in the treatment of parton distribution functions (PDFs). However, nuclear modification is not excluded within the precision of the measurement [7]. The production of Z bosons, examined as a function of centrality, was also found to scale with $\langle N_{\text{coll}} \rangle$.

To differentiate between initial- and final-state effects in heavy-ion collisions, the study of $p + \text{Pb}$ collisions is used at the LHC. One would expect that hot and dense QCD medium cannot be formed in such collisions, unlike in the $\text{Pb} + \text{Pb}$ case, and that modifications to final-state particles relative to nucleon-nucleon collisions should originate from the initial state of the nucleus. This assumption was challenged by the very first results from $p + \text{Pb}$ collisions at $\sqrt{s_{NN}} = 5.02$ TeV produced at the LHC in 2012. Results on multiparticle correlations, published for three LHC experiments [8–14], revealed collective behavior in $p + \text{Pb}$ collisions similar to that previously measured in heavy-ion collision systems. The yields of jets measured by ATLAS scale with $\langle N_{\text{coll}} \rangle$ when

measured inclusively for all centralities but show significant deviations from binary scaling when considered in centrality selections [15]. The CMS Collaboration has measured dijet pseudorapidity distributions and found them to agree better with predictions that include nuclear PDF modifications than with predictions that do not include nuclear effects [16]. The CMS Collaboration has also recently measured the production of W bosons in $p + \text{Pb}$ collisions and observed hints of nuclear modifications of the PDF [17]. Collectively, these results have highlighted the need for a better understanding of the initial conditions of $p + \text{Pb}$ collisions.

Unlike symmetric $\text{Pb} + \text{Pb}$ collisions, in $p + \text{Pb}$ collisions nuclear modifications of the PDFs in the lead nucleus create an asymmetry in the rapidity-dependent cross section of Z bosons; this presents an attractive observable for the study of initial-state nuclear conditions. The centrality-dependent yield of Z bosons is a well-suited probe to test our understanding of $p + \text{Pb}$ collision geometry. The LHCb Collaboration has made a first exploratory measurement of Z bosons at far forward and backward rapidities [18] based on an integrated luminosity of 1.6 nb^{-1} .

This paper presents the results of the measurement of Z boson production in $p + \text{Pb}$ collisions at $\sqrt{s_{NN}} = 5.02$ TeV using the ATLAS detector. The yield of Z bosons is measured as a function of their transverse momentum p_T^Z , rapidity in the center-of-mass frame (y_Z^*),¹ and centrality. The leptonic

*Full author list given at the end of the article.

¹ATLAS uses a right-handed coordinate system with its origin at the nominal interaction point in the center of the detector and the z axis along the beam pipe. The x axis points from the interaction point to the center of the LHC ring, and the y axis points upward. Cylindrical coordinates (r, ϕ) are used in the transverse plane, ϕ being the azimuthal angle around the beam pipe. The rapidity in the laboratory frame is given by $y^{\text{lab}} = \frac{1}{2} \ln \frac{E + p_z}{E - p_z}$ and pseudorapidity is defined as $\eta = -\ln[\tan(\theta/2)]$. Positive rapidity corresponds to the direction the proton beam travels, “proton-going,” and negative rapidity is referred to as “ Pb -going.” In this convention the asymmetric beam energies result in a center of mass shifted to rapidity, $y^* = y^{\text{lab}} - 0.465$.

decays of the Z boson ($Z \rightarrow ee$ and $Z \rightarrow \mu\mu$) are used for its reconstruction. In the muon channel it is possible to reconstruct the Z boson in the rapidity range $-3 < y_Z^* < 2$, while in the electron channel this range can be extended to $|y_Z^*| < 3.5$. The larger acceptance in rapidity for $Z \rightarrow ee$ candidates is possible because of the larger acceptance of the ATLAS calorimeters compared to the muon spectrometer (MS; Secs. II and III B). The efficiency of Z boson reconstruction is calculated from detector simulations (Sec. III D). Backgrounds in each channel are estimated using simulations and data-driven methods (Sec. III E). Results measured in the dimuon and dielectron decay channels are combined after accounting for uncertainties and their correlations (Sec. III G). The measured cross sections and centrality-dependent yields are compared to models of $p + Pb$ collisions composed of 82 pp and 126 pn collisions in which the production of Z bosons is obtained using perturbative QCD calculations.

II. THE ATLAS DETECTOR

The ATLAS detector [19] at the LHC covers nearly the entire solid angle around the collision point. It consists of an inner tracking detector surrounded by a thin superconducting solenoid, electromagnetic and hadronic calorimeters, and an MS.

The inner detector (ID) system is immersed in a 2-T axial magnetic field and provides charged particle tracking in the pseudorapidity range $|\eta| < 2.5$. It comprises a high-granularity silicon pixel detector covering the collision region, surrounded by a silicon microstrip tracker and a transition radiation tracker.

The calorimeters cover the range $|\eta| < 4.9$. Within the region $|\eta| < 3.2$, electromagnetic calorimetry is provided by barrel and endcap high-granularity lead liquid-argon (LAr) calorimeters, with an additional thin LAr presampler covering $|\eta| < 1.8$. Behind the electromagnetic calorimeter there is a steel/scintillator sampling hadronic calorimeter covering $|\eta| < 1.7$, and LAr hadronic calorimeters extend the coverage to $|\eta| < 4.9$. Forward electromagnetic calorimeters (FCals) are located in the range $3.1 < |\eta| < 4.9$. Electrons may be reconstructed over the entire electromagnetic calorimeter system, $|\eta| < 4.9$.

The MS comprises separate trigger and high-precision tracking chambers that measure the deflection of muons in a magnetic field generated by superconducting air-core toroids. The precision chambers cover the region $|\eta| < 2.7$ with three layers of monitored drift tube chambers, complemented by cathode strip chambers in the innermost layer of the forward region. The muon trigger system covers the range $|\eta| < 2.4$, with resistive plate chambers in the barrel ($|\eta| < 1.05$) and thin gap chambers in the endcap regions ($1.05 < |\eta| < 2.4$).

The ATLAS detector has a three-level trigger system [20]: the hardware-based level 1 (L1) trigger and the software-based high-level trigger, which is subdivided into the level 2 (L2) trigger and the event filter. Single-electron and single-muon triggers are used to acquire the data analyzed in this paper. Minimum-bias events are selected based on signals in the minimum-bias trigger scintillators (MBTS) that detect charged particles in the range $2.1 < |\eta| < 3.9$.

III. ANALYSIS

A. Data sample

This analysis uses the 2013 ATLAS $p + Pb$ collision data at $\sqrt{s_{NN}} = 5.02$ TeV, produced from a 4-TeV proton beam and a 1.57-TeV-per-nucleon lead beam. The asymmetric energy of the beams resulted in a shift of the center-of-mass by 0.465 units of rapidity relative to the laboratory frame. After 60% of the data were recorded the directions of the proton and lead beams were reversed. Results obtained in the two data periods are found to be consistent with each other. In this paper all data from both periods are presented using the convention that the proton beam travels *forward* in the positive-rapidity direction.

Following stringent data-quality requirements, the $Z \rightarrow ee$ and $Z \rightarrow \mu\mu$ analyses use samples corresponding to integrated luminosity values of 29.4 ± 0.8 and 28.1 ± 0.8 nb $^{-1}$, respectively. The luminosity measurement for the 2013 $p + Pb$ data is calibrated based on dedicated beam-separation scans. Systematic uncertainties similar to those studied for the calculation of pp luminosity [21] are calculated. The combination of these systematic uncertainties results in a total uncertainty in the ATLAS luminosity scale during proton-lead collisions at $\sqrt{s_{NN}} = 5.02$ TeV of 2.7%. Minimum-bias $p + Pb$ collisions were selected by a trigger based on a signal in both MBTS counters. Minimum-bias events are required to have the time measured in each MBTS be consistent within 10 ns and a reconstructed collision vertex within 175 mm of the nominal collision point in the longitudinal direction [22].

B. Lepton reconstruction

Electron candidates are first identified by the L1 trigger as a cluster of cells in the electromagnetic calorimeter, formed into $(\Delta\phi \times \Delta\eta) = 0.1 \times 0.1$ trigger towers, within the range $|\eta| < 2.5$ and with the cluster transverse energy exceeding 5 GeV. The high-level trigger then incorporates tracking information from the ID and imposes electron identification requirements on the electron candidates. A trigger for at least one electron candidate with $E_T > 15$ GeV and satisfying loose identification requirements is used to select events.

In the off-line analysis, electron candidates within $|\eta| < 4.9$ are selected using the ATLAS reconstruction algorithm [23]. Electrons with $|\eta| < 2.47$, referred to as midrapidity electrons, require the matching of a track to an energy cluster in the electromagnetic calorimeter. In addition to the reconstruction requirements, further electron identification selections based primarily on the shower shape in the electromagnetic calorimeter are made to reject background. Electron identification requirements used in previous ATLAS analyses [23] are used to provide quality classification of electrons based on the tightness of the identification criteria they satisfy. The triggering electron is required to have $E_T > 20$ GeV, to be outside the pseudorapidity interval $1.37 < |\eta| < 1.52$ (a transition region between the barrel and the endcap calorimeters which contains a relatively large amount of inactive material), and to satisfy tight identification quality requirements. If the other electron is within $|\eta| < 2.47$, it must have $E_T > 10$ GeV and satisfy looser quality requirements. Forward electrons are those reconstructed within the range $2.5 < |\eta| < 4.9$ based on energy deposited in the FCal [23]. There is no tracking

in this region, so the electron candidate reconstruction and identification are derived solely from the calorimeter signal and do not have an associated charge. Forward electrons are required to have $E_T > 20$ GeV. Of $Z \rightarrow ee$ decays with $|y_Z^*| < 3.5$, approximately 82% fall into the fiducial acceptance defined by the electron p_T and η requirements.

Muon candidates are first identified at the L1 trigger, based on hits in either the resistive plate chamber or the thin gap chamber. The high-level trigger then reconstructs muon tracks in the vicinity of the detector region reported by the L1 trigger. The L2 trigger uses an algorithm to perform a fast reconstruction of muons, which is then refined in the event filter by incorporating the hits in the ID tracking as well as those in the MS tracking. Events containing at least one muon with p_T greater than 8 GeV are accepted by the high-level trigger.

For the $Z \rightarrow \mu\mu$ analysis, muons are identified from candidates reconstructed in both the MS and the ID [24]. Muons are reconstructed separately in the MS and ID and a χ^2 -minimization procedure is used to obtain combined muon kinematic information. To reduce background from jets, each muon is required to pass a loose track-based isolation selection. Tracks are considered in a cone of size $\Delta R = \sqrt{(\Delta\eta)^2 + (\Delta\phi)^2} = 0.3$ around the direction of the muon. The muon is considered isolated if the scalar sum of the p_T of these tracks, excluding the muon, is less than 50% of the muon p_T . The efficiency of this selection is greater than 99%. The triggering muon is required to have $p_T > 20$ GeV and be within $|\eta| < 2.4$. The second muon must be within $|\eta| < 2.47$ and have $p_T > 10$ GeV. Approximately 68% of Z bosons with $-3 < y_Z^* < 2$ fall into the fiducial acceptance defined by the muon kinematic requirements.

C. Centrality

In addition to measuring the Z boson cross section, the Z boson yield per minimum-bias event is measured for different centrality selections. In order to characterize the $p + \text{Pb}$ collision geometry, each event is assigned a centrality based on the total transverse energy measured in the FCal on the Pb-going side ($-4.9 < \eta < -3.2$), ΣE_T^{FCal} [22]. Collisions with more (fewer) participating nucleons are referred to as central (peripheral). As in Ref. [22], the standard Glauber model [25] approach is used to calculate the mean number of participating nucleons, $\langle N_{\text{part}} \rangle$. The mean number of inelastic nucleon-nucleon collisions, $\langle N_{\text{coll}} \rangle$, is $\langle N_{\text{part}} \rangle - 1$. Based on the observed centrality dependence of the charged particle multiplicity [22], a Glauber-Gribov color fluctuation (GGCF) model [26,27], an extension to the Glauber model which allows event-by-event fluctuations of the nucleon-nucleon cross section $\sigma(N + N \rightarrow X)$, is also considered. In this model the magnitude of the fluctuations is characterized by the parameter ω_σ , with $\omega_\sigma = 0$ corresponding to the standard Glauber model. Following Ref. [22], two values of ω_σ , 0.11 and 0.2, based on the calculations in Refs. [26,27], are implemented and considered for this analysis.

Following Ref. [22], the centrality selections used for this analysis, in order from most central to most peripheral, are 0–5%, 5–10%, 10–20%, 20–30%, 30–40%, 40–60%, and

60–90%. For the study of the y_Z^* distribution as a function of centrality (see Sec. IV B), larger bins are used: 0–10%, 10–40%, and 40–90%. For the most peripheral collisions, centrality greater than 90%, centrality modeling, and associated geometric quantities are not well constrained. Pileup events, those containing multiple $p + \text{Pb}$ interactions from the same bunch crossing, are removed by rejecting events in which more than one primary vertex is reconstructed. The fraction of candidate events which is removed from the centrality-selected Z boson yield analysis due to pileup rejection is approximately 5%. Diffractive events are identified by a rapidity gap (defined by the absence of calorimeter energy clusters) of greater than two units on the Pb-going side of the detector and excluded. This leads to a rejection of less than 0.1% of Z boson candidate events. The total number of minimum-bias events corresponding to the luminosity sampled by the trigger, N_{evt} , is used to define the Z boson yield per event in each centrality selection.

Besides its sensitivity to the event geometry, the ΣE_T^{FCal} for a fixed geometry may also be affected by the presence of a hard scattering process in the event. In particular, the calculation of centrality for $Z \rightarrow ee$ events in which there is a forward electron in the Pb-going-side FCal is biased by the energy of the electron. This is corrected by subtracting the transverse energy of the electron from ΣE_T^{FCal} . The subtraction procedure is found to effectively recover the correct centrality of minimum-bias events into which simulated $Z \rightarrow ee$ decays containing electrons in the Pb-going-side FCal were overlaid.

In addition to the case where there is a Z -decay electron in the Pb-going-side FCal, ΣE_T^{FCal} may be more subtly biased in all Z boson events. The presence of a Z boson (or any hard process) is correlated with a higher transverse energy of the underlying event. Consequently, more energy may be deposited in the Pb-going-side FCal in events containing a hard scattering process than in those that do not contain one. This causes a bias in the centrality-dependent yield, as the Z boson yield is enhanced in the more central events but depleted in the more peripheral ones. This effect, referred to as a centrality bias, has been noted for yields of hard processes in $d + \text{Au}$ collisions at $\sqrt{s_{NN}} = 200$ GeV by the PHENIX Collaboration [28] and in $p + \text{Pb}$ collisions at $\sqrt{s_{NN}} = 5.02$ TeV by the ALICE Collaboration [29].

A correction to the centrality-dependent yields of hard processes in $d + \text{Au}$ collisions at $\sqrt{s_{NN}} = 200$ GeV has been studied by the PHENIX Collaboration [28] (the correction is also calculated for $p + \text{Pb}$ at $\sqrt{s_{NN}} = 5.02$ TeV). The centrality bias correction used by the PHENIX Collaboration is based on the modeling of an increase in the mean particle multiplicity produced by the specific NN collision that undergoes a hard scattering. Recently, similar calculations of a centrality bias have been made in which all NN collisions may contribute to an increase in the particle multiplicity [30]. The increase in multiplicity stemming from each NN collision is taken to be proportional to the contribution from that collision to the E_T in the event. This model is applied to the ATLAS $p + \text{Pb}$ centrality classification for the standard Glauber analysis as well as the GGCF models and, thus, used to calculate corrections to the hard process yield measured in a given centrality bin. Because the N_{part} probability distribution varies

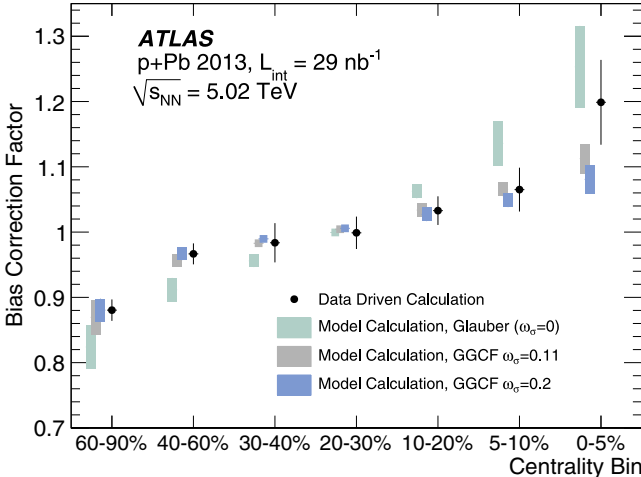


FIG. 1. (Color online) Centrality bias correction factors and their uncertainties (bars), from Ref. [30], for the Glauber and GGCF model configurations, and bias correction factors derived from data (points) as explained in the text. The reciprocals of the correction factors are applied as multiplicative factors to the centrality-dependent Z boson yields.

less steeply in the GGCF models than in the standard Glauber model, the centrality bias corrections are closer to unity for the GGCF cases. The corrections from Ref. [30] are shown in Fig. 1. The reciprocals of the corrections are applied as multiplicative factors to the centrality-dependent Z boson yields measured in the present analysis.

Using Z bosons measured in ATLAS, data-driven centrality bias corrections may be calculated and compared with the results in Ref. [30]. To do so, the corrections are calculated by comparing the transverse energy deposited in the FCal in events selected by the minimum-bias trigger and in Z boson events from pp collisions (in which there is no centrality to consider). This effect is studied in pp collisions at $\sqrt{s} = 2.76$ TeV and $\sqrt{s} = 7$ TeV from the 2011 LHC run. At both energies a significant increase in the mean transverse energy deposited in the FCal is observed and, within the uncertainties of the measurement, found to be independent of the Z boson kinematics. A single value is interpolated from the $\sqrt{s} = 2.76$ TeV and $\sqrt{s} = 7$ TeV data for $\sqrt{s_{NN}} = 5.02$ TeV. The interpolation is performed using both logarithmic and linear expressions, and the difference between them contributes to the systematic uncertainty. A correction is made to account for the shifted center of mass in the $p + Pb$ system, which changes the effective FCal acceptance in η compared to pp . From this procedure an additive shift to ΣE_T^{FCal} of 2.0 ± 0.5 GeV is calculated. In each $p + Pb$ $Z \rightarrow \ell\ell$ event this value is subtracted from ΣE_T^{FCal} and the resulting value used to determine a corrected centrality of the event. The centrality-dependent yield may be constructed, according to the method described in Sec. III E, using both the subtracted and the unsubtracted ΣE_T^{FCal} values and their ratio is then comparable to a centrality bias correction factor that may be compared to those calculated in Ref. [30]. As shown in Fig. 1, within the uncertainties this data-based method is compatible with the model calculations.

D. Monte Carlo (MC) simulation corrections

The trigger, reconstruction, and identification efficiencies of electrons and muons as well as the muon isolation efficiency are evaluated by an MC simulation complemented by data-driven estimates of these quantities. Using the POWHEG generator [31] (with the CT10 PDF [32]) interfaced to PYTHIA8 [6] for simulation of the parton shower, approximately 10 million $Z \rightarrow ee$ and 4 million $Z \rightarrow \mu\mu$ events were simulated. The Z bosons were generated from pp and pn collisions, which were added together with weights 82/208 and 126/208, respectively, corresponding to the numbers of protons and neutrons in the Pb ion. The response of the ATLAS detector to the generated particles was modeled using GEANT4 [33,34]. Due to the dependence of electron identification and reconstruction efficiency on the detector occupancy, simulated $Z \rightarrow ee$ events were overlaid with data events selected with the minimum-bias trigger and then reconstructed.

To cross-check the efficiencies calculated in the MC simulation, a “tag-and-probe” technique is employed. The tag is defined as a fully reconstructed high-quality triggered lepton, whereas the probe is a lepton candidate to which triggering, reconstruction, or quality requirements are not applied. Using tag-and-probe pairs with an invariant mass $m_{\ell\ell}$ consistent with selection of Z bosons, the efficiency of the probe with additional requirements is calculated. The mass window used depends on the background present in the probe sample and ranges from $80 < m_{\ell\ell} < 100$ to $87 < m_{\ell\ell} < 95$ GeV. For example, the electron trigger efficiency is measured from high-quality reconstructed electron probes selected without an *a priori* trigger requirement, and the MS reconstruction efficiency is measured from charged-particle tracks in the ID without an *a priori* MS signal requirement. The MC simulation is scaled to match the efficiencies determined with the data-driven tag-and-probe method. The factors used to scale the MC electron response are derived from the 2013 $p + Pb$ data set. Muon reconstruction is insensitive to the differences between 2013 $p + Pb$ and 2012 pp conditions and therefore the scale factors for muons are taken from $Z \rightarrow \mu\mu$ events collected in the 2012 pp data set [24]. The scale factors for the $Z \rightarrow ee$ ($Z \rightarrow \mu\mu$) MC events deviate from unity by less than 5% (1%).

The trigger efficiencies of electrons and muons depend on η and have average values of approximately 95% and 83%, respectively. The reconstruction and identification efficiency of the more stringently selected electrons is approximately 75%, whereas the reconstruction and identification efficiency for the looser-quality midrapidity electrons is approximately 88% and the forward-electron efficiency is about 65%. These values depend on η and p_T . The muon reconstruction efficiency is approximately 95%, depending on η .

Correction factors for the yields of $Z \rightarrow ee$ and $Z \rightarrow \mu\mu$ candidates are calculated from the MC simulations as functions of p_T^Z , y_Z^* , and $p + Pb$ centrality. These corrections take into account the cumulative losses due to the trigger, reconstruction, and identification efficiency as well as the kinematic acceptance of decay leptons. The correction is defined relative to all generated Z bosons within the mass window $66 < m_{\ell\ell} < 116$ GeV. The total efficiency for reconstructing a produced Z boson, including acceptance, is approximately 55% for

$Z \rightarrow ee$ and 65% for $Z \rightarrow \mu\mu$. Following the subtraction of background (see Sec. III E) and application of the correction factor, a corrected yield of Z bosons is obtained in each bin of p_T^Z and y_Z^* . The uncertainty of the correction factor follows from the uncertainty of the data-driven tag-and-probe checks of the MC, primarily due to the relatively low number of tag-and-probe events in the data. The uncertainty associated with the lepton identification efficiency is the dominant uncertainty for both the $Z \rightarrow ee$ and the $Z \rightarrow \mu\mu$ analyses. This uncertainty is approximately 10% for $Z \rightarrow ee$ (rising as high as 15% for pairs including a forward electron) and 1.5% for $Z \rightarrow \mu\mu$. The sizable uncertainty for $Z \rightarrow ee$ is primarily driven by the limited size of the tag-and-probe 2013 $p + \text{Pb}$ data set. The other uncertainties are typically less than 2% in both channels.

E. Yield extraction

To form $Z \rightarrow ee$ candidates, all electrons found in triggered events are paired with each other. When both electrons are at midrapidity ($|\eta| < 2.47$), the unlike-sign charged pairs with an invariant mass satisfying $66 < m_{ee} < 116$ GeV are accepted as signal Z boson candidates. The like-sign pairs in this window are used to estimate the combinatorial background, created primarily by jets. In total, 1647 unlike-sign pairs and 52 like-sign pairs are reconstructed. The like-sign pairs are composed of combinatorial background and $Z \rightarrow ee$ decays in which one of the electrons has misreconstructed charge. The contribution from pairs with misreconstructed charge is estimated, using the MC simulation, to be half of the like-sign pairs, and the remainder is taken as an estimate of the background. Pairs made of one midrapidity electron and one nontriggering forward electron have a larger contribution from background and so an invariant mass window of $80 < m_{ee} < 100$ GeV is used to select Z boson candidates. To facilitate combination of all $Z \rightarrow ee$ candidates, an acceptance correction is made to account for the smaller mass window. No charge requirement is made for these candidates because the nontriggering electron is outside the acceptance of the ID and therefore does not have a reconstructed charge. There are 264 such candidates, of which an estimated 5% are background based on a fit of the invariant mass distribution. The fit is performed in the range $60 < m_{ee} < 120$ GeV using a signal shape from the MC simulation and several background parametrizations assuming exponential or polynomial descriptions of the background. The mass distributions of $Z \rightarrow ee$ candidates are shown in Figs. 2(a) and 2(b), along with the reconstructed MC simulation of the same quantity. The estimated background is subtracted from the signal candidates differentially in rapidity, transverse momentum, and centrality.

A similar procedure is also followed to select $Z \rightarrow \mu\mu$ candidates with an invariant mass of $66 < m_{\mu\mu} < 116$ GeV. This selection yields 2032 unlike-sign charged candidates and 4 like-sign pairs; their mass distribution is shown in Fig. 2(c). The MC simulation describes the data well in both lepton channels. The slight shift of the mass peak visible between the data and the simulation for dielectron events has only a very small effect on the calculation of corrections based on the MC simulation and is incorporated into the systematic uncertainty associated with electron reconstruction.

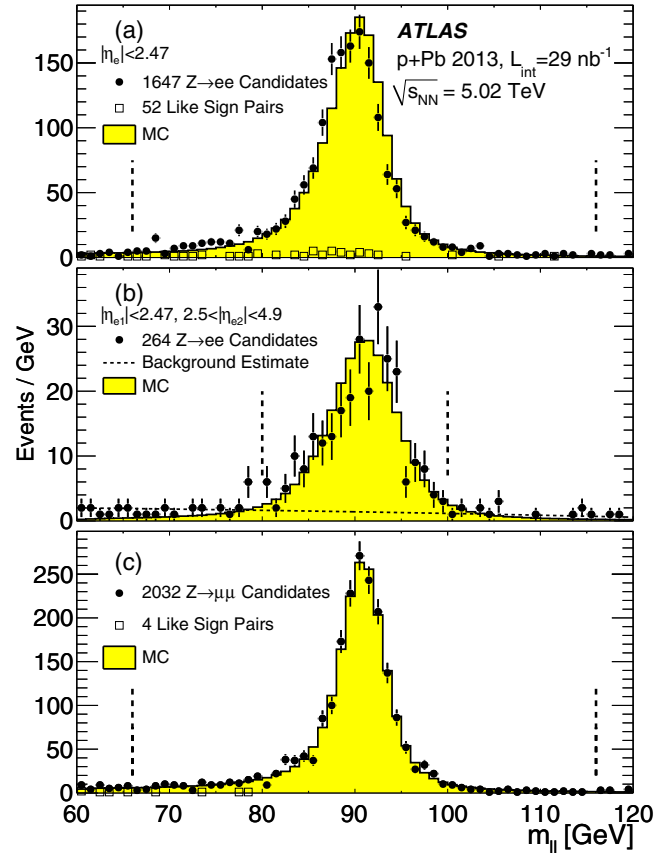


FIG. 2. (Color online) Dilepton invariant mass distributions in data and MC simulation. (a) $Z \rightarrow ee$ candidates with both electrons at midrapidity ($|\eta| < 2.47$); (b) candidates in which the nontriggering electron is a forward electron ($2.5 < |\eta| < 4.9$); (c) $Z \rightarrow \mu\mu$ candidates. The midrapidity $Z \rightarrow ee$ and $Z \rightarrow \mu\mu$ distributions are overlaid with the mass distributions of like-sign lepton pairs. For candidates in which the nontriggering electron is a forward electron ($2.5 < |\eta| < 4.9$) the background, estimated based on a decomposition of the invariant mass distribution (see text), is shown. In all plots the vertical lines indicate the mass window within which candidates are defined, and the MC simulation is normalized to the data inside this region.

Based on the like-sign pairs and MC simulation of charge misreconstruction, the uncertainty from the background subtraction is approximately 1% in the $Z \rightarrow ee$ channel for pairs in which both electrons are at midrapidity; in pairs involving a forward electron the uncertainty ranges from 5% to 20% based on fits of the invariant mass distribution. The background uncertainty in the $Z \rightarrow \mu\mu$ yield is negligible. The largest source of correlated background in both lepton decay channels is the decay of $Z \rightarrow \tau\tau$ events into dielectron and dimuon pairs. These are simulated and reconstructed just as $Z \rightarrow ee$ and $Z \rightarrow \mu\mu$ are but are found to have a negligible contribution following the analysis procedures.

F. Systematic uncertainties

The dominant source of uncertainty in the $Z \rightarrow ee$ measurement stems from imperfect knowledge of the efficiency

TABLE I. Relative systematic uncertainties (in percent) associated with the measurement of $Z \rightarrow ee$. The uncertainties typically increase at the more forward rapidities. Background includes charge misreconstruction, and electron reconstruction includes resolution. The last two rows refer only to pairs where one of the electrons was reconstructed in the range $3.1 < |\eta| < 4.9$.

Source	Uncertainty range (%)
Electron ID	6–14
Electron reconstruction	1–3
Electron trigger	1–2
Background	1–3
MC y_Z^* shape	0–2
Forward-electron reconstruction	4–15
Forward-electron background	2–10

of the electron identification requirements. The uncertainty is driven by the limited number of events available for the tag-and-probe analysis, which had to rely on 2013 $p + Pb$ collision data because the electron reconstruction performance changed due to detector conditions and occupancy compared to earlier pp collision data. The uncertainty is larger in pairs involving a forward-electron, and the sample has a lower purity than the sample of midrapidity electrons. Other electron uncertainties are significantly smaller and are associated with the trigger efficiency, electron reconstruction efficiency and energy resolution, background subtraction (which becomes significant for forward electrons), and charge misreconstruction. In addition, a small uncertainty stems from possible differences between the simulated y_Z^* distribution and the one measured in the data. The $Z \rightarrow ee$ systematic uncertainties depend on p_T^Z , y_Z^* , and $p + Pb$ centrality and are summarized in Table I.

The conditions of muon reconstruction in the 2013 $p + Pb$ collision data closely resemble those in pp collisions described in Ref. [24]. The small uncertainties from the more abundant pp data are used in this analysis. An uncertainty of 1%, based on the performance of the muon reconstruction in high-pileup pp collisions, is associated with the scale factors to account for possible differences between the data sets. The uncertainties depend on p_T^Z and y_Z^* . Table II summarizes the systematic uncertainties of the $Z \rightarrow \mu\mu$ measurement.

In addition to the Z boson measurement uncertainties, a 2.7% uncertainty is associated with the luminosity calculation. For the centrality-dependent yields that are scaled by $\langle T_{AA} \rangle$ the uncertainties of the Glauber model calculations are taken

TABLE II. Relative systematic uncertainties (in percent) associated with the measurement of $Z \rightarrow \mu\mu$.

Source	Uncertainty range (%)
Muon ID & reconstruction	1.5
Muon trigger	1–2
Background	<1
p_T resolution	<1
MC y_Z^* shape	<1.5

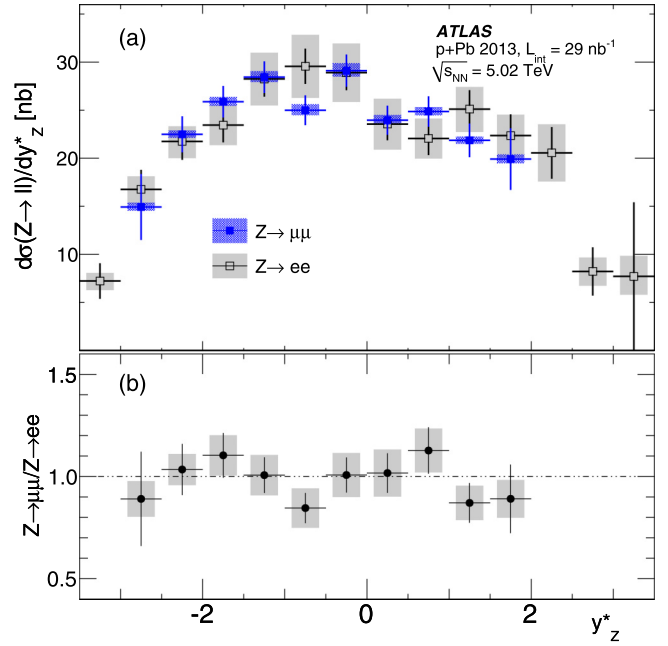


FIG. 3. (Color online) (a) Differential Z boson production cross section, $d\sigma/dy_Z^*$, as a function of Z boson rapidity in the center-of-mass frame y_Z^* , for $Z \rightarrow ee$ and $Z \rightarrow \mu\mu$. (b) Their ratio. Bars indicate statistical uncertainty; shaded boxes, systematic uncertainty.

from Ref. [22]. The correction to centrality due to bias from the presence of a hard scattering, taken from Ref. [30], has uncertainties as shown in Fig. 1.

G. Lepton channel combination

The cross section in each leptonic decay channel is defined for the mass window $66 < m_Z < 116$ GeV, the rapidity ranges $|y_Z^*| < 3.5$ for $Z \rightarrow ee$ and $-3 < y_Z^* < 2$ for $Z \rightarrow \mu\mu$, and the full decay lepton kinematic phase space. The $Z \rightarrow ee$ and $Z \rightarrow \mu\mu$ yields, corrected for acceptance and efficiency, are used to calculate the cross section in each channel, and a good agreement between the two is observed as shown for the y_Z^* distributions in Fig. 3.

The two decay channel results are combined to one set of $Z \rightarrow \ell\ell$ data using the method described in Refs. [35,36]. The technique uses a χ^2 minimization procedure with a nuisance parameter formalism to combine the data sets coherently. The procedure distinguishes those systematic uncertainty sources that are uncorrelated bin to bin, uncorrelated across data sets, and fully correlated bin to bin and across data sets. In this way, combined points are calculated to optimize the overall agreement of the data sets, given the correlation of the uncertainties. This may result in differences in the combined $Z \rightarrow \ell\ell$ data points relative to the $Z \rightarrow ee$ data points in rapidity regions in which there are no $Z \rightarrow \mu\mu$ data points. Following this, an integrated cross section for the region $|y_Z^*| < 3.5$ is defined for the combined $Z \rightarrow \ell\ell$ points based on both the $Z \rightarrow ee$ and the $Z \rightarrow \mu\mu$ data even though the $Z \rightarrow \mu\mu$ data are limited to $-3 < y_Z^* < 2$. The systematic uncertainties associated with the combined results are fully correlated bin to bin in each distribution. They are

TABLE III. The measured integrated cross section (in nb) for several rapidity ranges, for $Z \rightarrow \mu\mu$, $Z \rightarrow ee$, and the combined $Z \rightarrow \ell\ell$. The first uncertainty listed is statistical, and the second systematic. There is an additional 2.7% luminosity uncertainty for each cross section. Cross sections predicted by the models (see text) are also listed. Uncertainties listed with the model calculations are the PDF and scale uncertainties added in quadrature.

y_Z^*	[-2,0]	[0,2]	[-3,2]	[-3.5,3.5]
$Z \rightarrow \mu\mu$	$54.2 \pm 1.6 \pm 1.3$	$45.3 \pm 2.1 \pm 0.9$	$118.2 \pm 3.3 \pm 2.6$	N/A
$Z \rightarrow ee$	$55.1 \pm 1.8 \pm 5.9$	$46.5 \pm 2.2 \pm 5.0$	$121 \pm 3 \pm 13$	$143 \pm 5 \pm 17$
$Z \rightarrow \ell\ell$	$54.4 \pm 1.3 \pm 1.4$	$45.9 \pm 1.4 \pm 1.4$	$119.3 \pm 2.2 \pm 3.4$	$139.8 \pm 4.8 \pm 6.2$
CT10 (NLO)	47.4 ± 0.9	46.8 ± 0.9	110.8 ± 2.9	132.2 ± 3.3
CT10 + EPS09 (NLO)	48.7 ± 1.0	43.5 ± 1.1	108.6 ± 3.1	127.4 ± 3.6
MSTW2008 (NNLO)	$48.3^{+1.2}_{-0.9}$	$47.9^{+1.2}_{-0.9}$	$113.5^{+2.8}_{-2.2}$	$135.2^{+3.4}_{-2.7}$

approximately 3% at midrapidity and rise to about 10% at forward and backward rapidity.

IV. RESULTS

A. $Z \rightarrow \ell\ell$ cross section

From the combined $Z \rightarrow ee$ and $Z \rightarrow \mu\mu$ data a total cross section of 139.8 ± 4.8 (statistical) ± 6.2 (systematic) ± 3.8

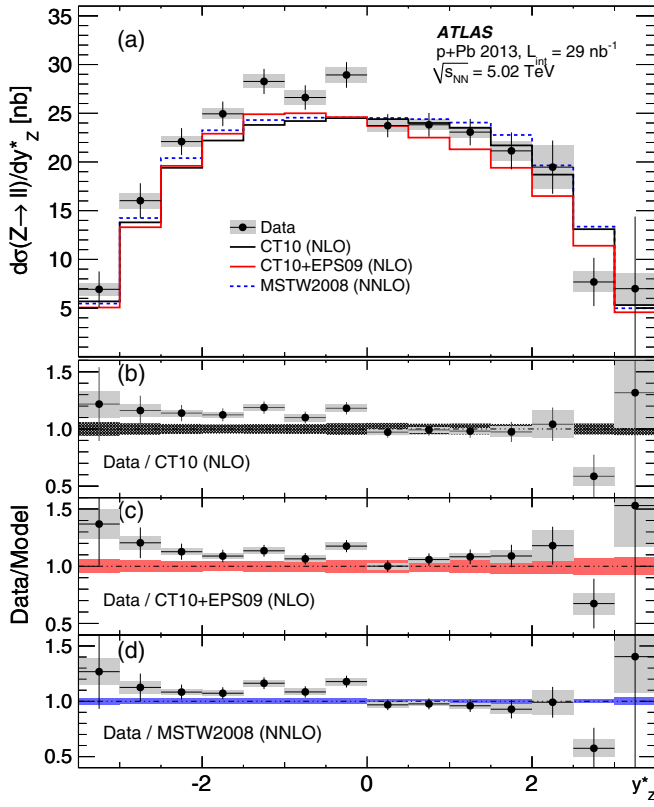


FIG. 4. (Color online) (a) The $d\sigma/dy_Z^*$ distribution from $Z \rightarrow \ell\ell$, shown along with several model calculations in the upper panel. Bars indicate statistical uncertainty, and shaded boxes systematic uncertainty, of the data; uncertainties of model calculations are not shown. (b)–(d) Ratios of the data to the models. Uncertainties of the model calculations (scale and PDF uncertainties added in quadrature) are shown as bands around unity in each panel. An additional 2.7% luminosity uncertainty of the cross section is not shown.

(luminosity) nb is obtained in the $|y_Z^*| < 3.5$ acceptance. Based on the MC simulation (and the models discussed below) this acceptance covers approximately 99.5% of the total $Z \rightarrow \ell\ell$ cross section. Restricting the results to the smaller rapidity interval of $-3 < y_Z^* < 2$, the cross section is 119.3 ± 2.2 (statistical) ± 3.4 (systematic) ± 3.2 (luminosity) nb. Table III lists the integrated cross section in the larger and

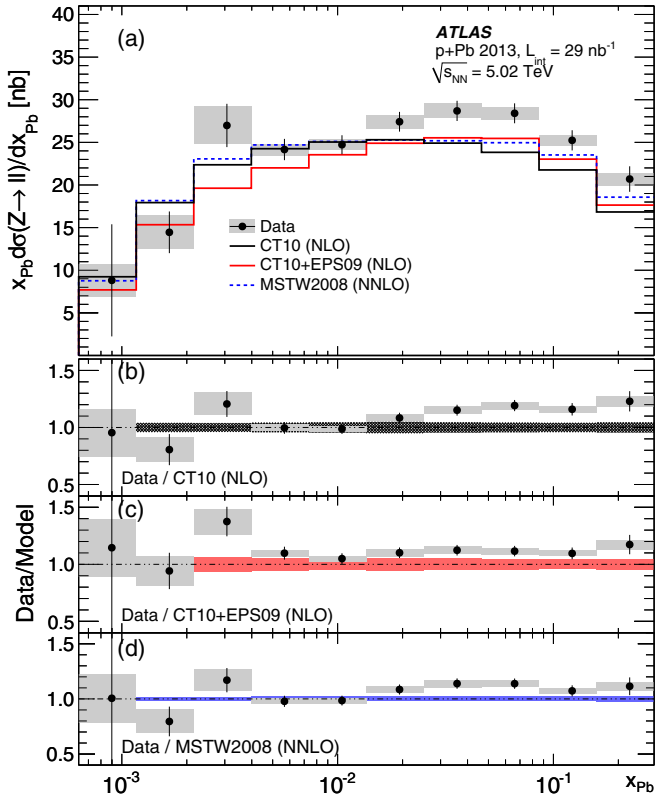


FIG. 5. (Color online) (a) The differential cross section of Z boson production multiplied by the Bjorken x of the parton in the lead nucleus, $x_{\text{Pb}} d\sigma/dx_{\text{Pb}}$, as a function of x_{Pb} using $Z \rightarrow \ell\ell$ events shown along with several model calculations. Bars indicate statistical uncertainty, and shaded boxes systematic uncertainty, of the data; uncertainties of the model calculations are not shown. (b)–(d) Ratios of the data to the models. Uncertainties of the model calculations are shown as bands around unity in each panel. There is an additional 2.7% luminosity uncertainty of the cross section.

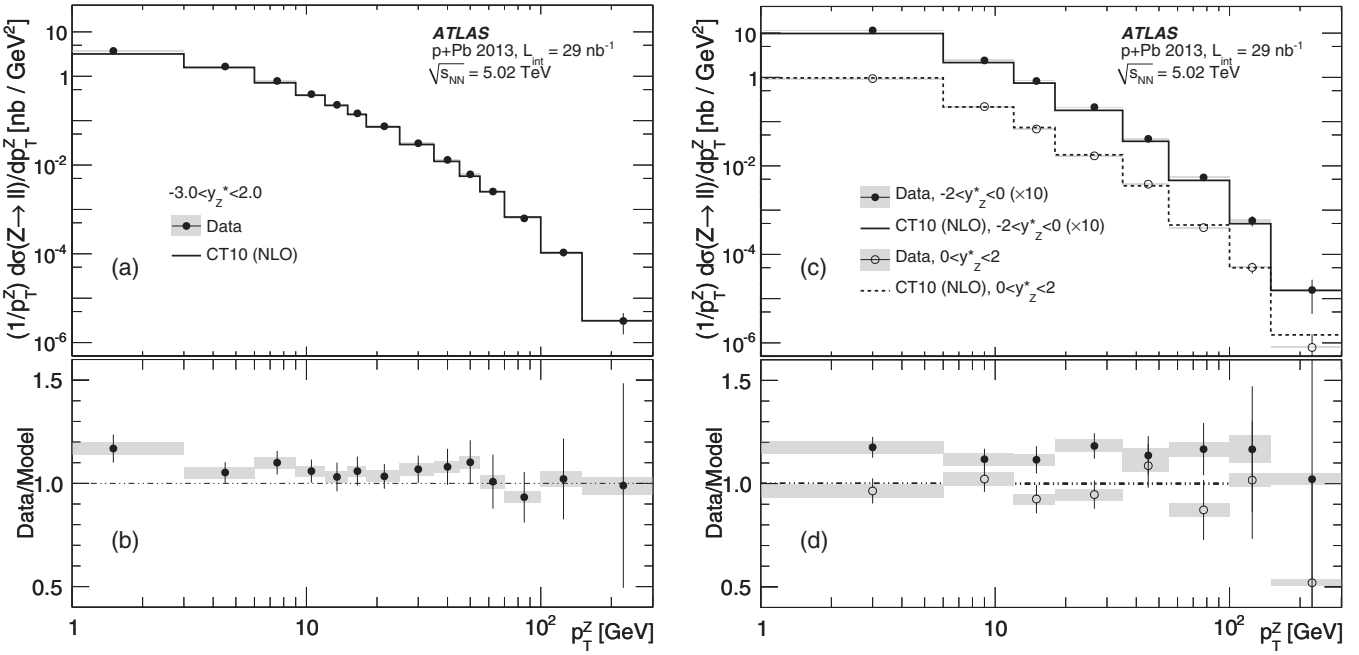


FIG. 6. (a), (c) Distributions of the differential cross section of Z boson production as a function of the transverse momentum of the Z , p_T^Z , shown along with the CT10 model calculation. (b), (d) Ratio of the data to the model. (a), (b) For $-3 < y_Z^* < 2$; (c), (d) for $-2 < y_Z^* < 0$ and $0 < y_Z^* < 2$. Bars indicate statistical uncertainty; shaded boxes, systematic uncertainty. The leftmost bin represents the range $0\text{--}3 \text{ GeV}$. An additional 2.7% luminosity uncertainty of the cross section is not shown.

smaller rapidity ranges as measured for each channel and their combination.

The measured cross section may be compared to a $p + \text{Pb}$ model prediction composed of a linear sum of the nucleon-nucleon cross sections: $82\sigma(pp \rightarrow Z + X) + 126\sigma(pn \rightarrow Z + X)$, corresponding to the numbers of protons and neutrons in the Pb ion. The value of $\sigma(pn \rightarrow Z + X)$ is 2% higher than that of $\sigma(pp \rightarrow Z + X)$ in all models discussed below. Calculating the baseline nucleon-nucleon cross sections using the CT10 PDF at NLO, as in the corresponding MC simulation, the model yields values of $132.2 \pm 3.3 \text{ nb}$ in the range $|y_Z^*| < 3.5$ and $110.8 \pm 2.9 \text{ nb}$ for $-3 < y_Z^* < 2$, where the uncertainties are the sums in quadrature of PDF and scale (renormalization and factorization) uncertainties. Using the MSTW2008 PDF, calculated with FEWZ [37] at next-to-next-to-leading order (NNLO), cross sections of $135.2^{+3.4}_{-2.7} \text{ nb}$ are obtained for $|y_Z^*| < 3.5$ and $113.5^{+2.8}_{-2.2} \text{ nb}$ for $-3 < y_Z^* < 2$. At NLO the results from MSTW2008 are very close to the CT10 results. In addition to the simple model of the $p + \text{Pb}$ Z boson cross section as a linear sum of nucleon-nucleon cross sections, calculations are performed incorporating nuclear corrections of the PDF. Including the EPS09 modifications [38] to the CT10 PDF results in cross sections of 127.4 ± 3.6 and $108.6 \pm 3.1 \text{ nb}$, respectively.

For a more detailed understanding of Z boson production, the measured cross section as a function of the Z boson rapidity is presented in Fig. 4 and compared to model calculations. The data are seen to be strongly asymmetric about $y_Z^* = 0$. The CT10 + EPS09 calculations come closest to reproducing the shape of the measured y_Z^* differential cross section. A χ^2 test of compatibility between the data and the

model shapes (irrespective of normalization) finds that the CT10 + EPS09 shape of the y_Z^* distribution gives a p value of 0.79. The unmodified CT10 calculation and MSTW2008 calculations have p values of 0.07 and 0.01, respectively. A Kolmogorov-Smirnov test was also performed and resulted in probabilities of 0.96, 0.09, and 0.07 for CT10 + EPS09, CT10, and MSTW2008 model calculations. This is consistent with the preference for the observation of nuclear correction effects as in the χ^2 test.

Nuclear modification of PDFs is fundamentally related to the Bjorken x of the relevant parton. At leading order, x_p in the proton and x_{Pb} in the lead nucleus are related to the reconstructed Z boson kinematics by

$$x_p = \frac{m_{ll} e^{y_Z^*}}{\sqrt{s_{\text{NN}}}}, \quad x_{\text{Pb}} = \frac{m_{ll} e^{-y_Z^*}}{\sqrt{s_{\text{NN}}}}. \quad (1)$$

The resulting x_{Pb} distribution is shown in Fig. 5 and compared to model calculations.

Figure 6 shows the p_T^Z distributions for $-3 < y_Z^* < 2$ and, separately, for $-2 < y_Z^* < 0$ and $0 < y_Z^* < 2$. These are compared to the baseline CT10 model. The p_T^Z dependence is less sensitive to nuclear effects and a good agreement between the experimental measurement and the MC simulation shape is observed.

B. Centrality-dependent yield

Results are presented for the centrality-dependent Z boson yield. If the rate of Z boson production were consistent with geometric expectations, then the Z boson yield divided by $\langle N_{\text{coll}} \rangle$ should be independent of centrality. To investigate

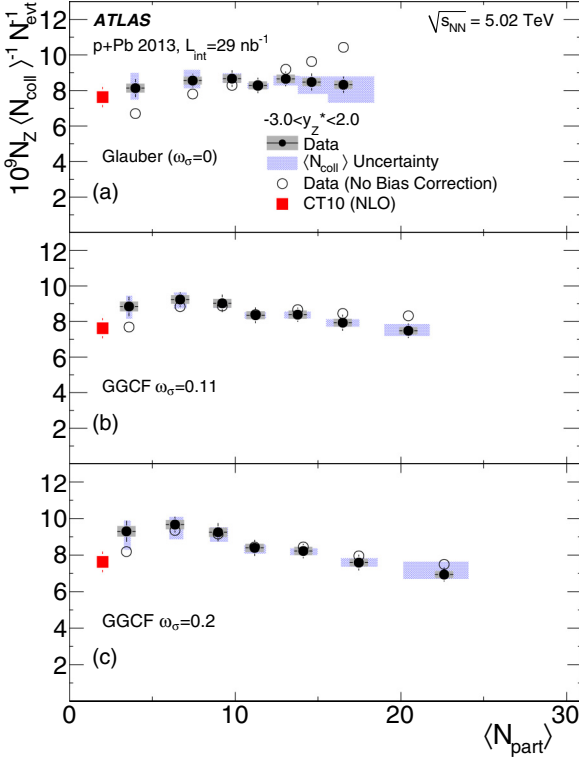


FIG. 7. (Color online) The yield of Z bosons per event scaled by the mean number of nucleon-nucleon collisions ($\langle N_{\text{coll}} \rangle$) as a function of the mean number of participating nucleons ($\langle N_{\text{part}} \rangle$). Each panel uses a different Glauber model configuration in calculating ($\langle N_{\text{part}} \rangle$) (and ($\langle N_{\text{coll}} \rangle$)). Standard Glauber model (a) with no Glauber-Gribov color fluctuations (GGCFs) and $\omega_\sigma = 0.11$ and (b) with GGCFs and $\omega_\sigma = 0.2$. The data are compared to the CT10 model prediction plotted at $\langle N_{\text{part}} \rangle = 2$. Bars indicate statistical uncertainty; shaded boxes, systematic uncertainty. Systematic uncertainties are correlated bin by bin. The ($\langle N_{\text{coll}} \rangle$) uncertainty plotted does not include the bin-by-bin fully correlated uncertainty stemming from the uncertainty of $\sigma(N + N \rightarrow X)$, which is instead included in the CT10 prediction uncertainty. As a reference, data are plotted as they would be with no centrality bias correction in the open points.

this, the yield of Z bosons per event scaled by $\langle N_{\text{coll}} \rangle$, within $-3 < y_Z^* < 2$, is displayed as a function of $\langle N_{\text{part}} \rangle$ in Fig. 7. The yield is independent of centrality defined using the standard Glauber model. Using the GGCF centrality models increases $\langle N_{\text{coll}} \rangle$ in central events and reduces it in peripheral events; consequently, the yield divided by $\langle N_{\text{coll}} \rangle$ is reduced in central events and increased in peripheral events. Figure 7 also shows the yield without the application of the centrality bias corrections discussed in Sec. III C.

The ATLAS Collaboration has previously measured the inclusive charged-hadron multiplicity in $p + \text{Pb}$ collisions as a function of centrality [22], and the centrality dependence of that quantity is similar to that observed in the present measurement. In order to quantify the similarity, the ratio $(dN_Z/dy^*)/(dN_{\text{ch}}/d\eta)$ is plotted vs $\langle N_{\text{part}} \rangle$ in Fig. 8. The charged-particle yield is expected to scale with $\langle N_{\text{part}} \rangle$ and the Z boson yield with $\langle N_{\text{coll}} \rangle = \langle N_{\text{part}} \rangle - 1$, and so the ratio is fit to a function with the form $a \cdot ((\langle N_{\text{part}} \rangle - 1)/\langle N_{\text{part}} \rangle)$. This

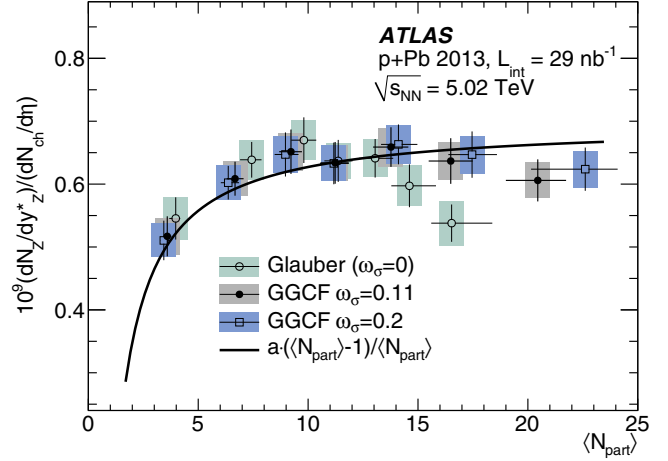


FIG. 8. (Color online) Ratio of the Z boson multiplicity to the inclusive charged particle multiplicity, $(dN_Z/dy^*)/(dN_{\text{ch}}/d\eta)$, as a function of $\langle N_{\text{part}} \rangle$. A function of the form $a \cdot ((\langle N_{\text{part}} \rangle - 1)/\langle N_{\text{part}} \rangle)$ is also shown. The normalization a is set based on the GGCF with $\omega_\sigma = 0.11$ points. Statistical uncertainties are plotted as bars; systematic uncertainties are plotted as shaded boxes.

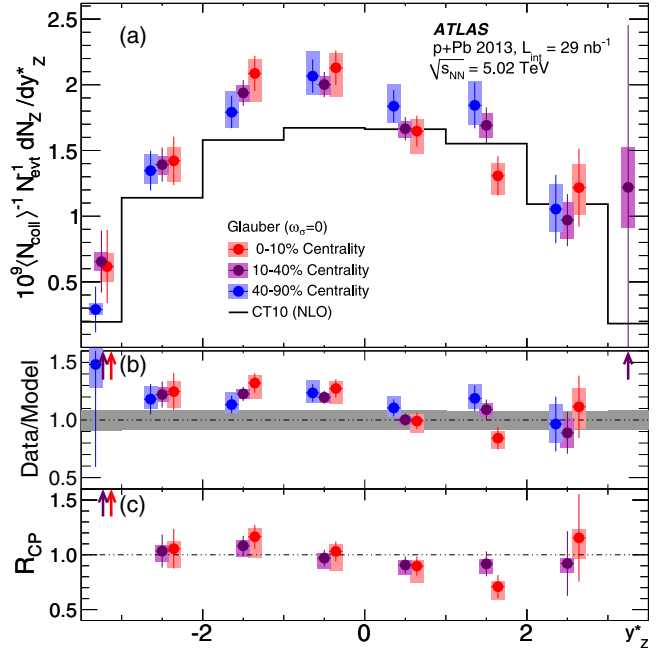


FIG. 9. (Color online) (a) Rapidity differential Z boson yields, scaled by $\langle N_{\text{coll}} \rangle$, for three centrality ranges compared with the CT10 model calculation. Bars indicate statistical uncertainty; shaded boxes, systematic uncertainty. The $\langle N_{\text{coll}} \rangle$ is defined with the standard Glauber model ($\omega_\sigma = 0$). The scale uncertainty stemming from the centrality calculation for each bin is included in the systematic uncertainty. Uncertainty associated with the model is not plotted. (b) Ratios of the data to the model. The uncertainty of the model added in quadrature to the scale uncertainty due to uncertainty in the inclusive NN cross section is shown as a band around unity. (c) R_{CP} (see text for details). The 0–10% and 40–90% centrality points are offset for visual clarity. Arrows in (b) and (c) indicate values outside the plotted axes.

function describes the data well for the GGCF cases, and less so for the standard Glauber model.

To further investigate the behavior observed in the rapidity differential cross section, the y_Z^* dependence of the Z boson yield in different centrality bins is also measured, as shown in Fig. 9. The differences between the data and the model are larger in central collisions. The $\langle N_{\text{coll}} \rangle$ -scaled ratio of central to peripheral data, R_{CP} , defined as

$$R_{\text{CP}}(y_Z^*) = \frac{\langle N_{\text{coll}} \rangle_{\text{peripheral}}}{\langle N_{\text{coll}} \rangle_{\text{central}}} \times \frac{dN_Z^{\text{central}}/dy_Z^*}{dN_Z^{\text{peripheral}}/dy_Z^*}, \quad (2)$$

is used to observe changes in the rapidity distribution for different centrality bins in a model-independent way and is shown in Fig. 9. Events with 40–90% centrality define the peripheral event selection, and two central selections, 0–10% and 10–40%, are compared with it. A linear fit of the $R_{\text{CP}}(y_Z^*)$ for 0–10% centrality results in a slope of -0.11 ± 0.04 , which suggests that the y_Z^* distribution may be different in most central events compared to peripheral events. For 10–40% centrality, the slope is -0.05 ± 0.03 .

V. SUMMARY

The Z boson production cross section has been measured in $p + \text{Pb}$ collisions at $\sqrt{s_{\text{NN}}} = 5.02 \text{ TeV}$ with the ATLAS detector at the LHC, using $Z \rightarrow ee$ ($Z \rightarrow \mu\mu$) decays in a 29.4-nb^{-1} (28.1-nb^{-1}) data sample. It is found to be slightly higher than predictions based on perturbative QCD calculations. Disregarding the difference in overall normalization, the shapes of the y_Z^* - and x_{Pb} -dependent cross sections are somewhat better described by models that include nuclear modification of the lead nucleus PDF compared to those that do not, although models without nuclear modification are not excluded. Following the application of a centrality bias correction, the centrality-dependent yield is found to scale with $\langle N_{\text{coll}} \rangle$. In addition, the centrality dependence of the y_Z^* distribution was studied, and the asymmetry in y_Z^* was found

to be slightly larger in more central events. Integrated over y_Z^* , the centrality dependence appears to be consistent with binary scaling and is similar to the production of inclusive charged particles.

ACKNOWLEDGMENTS

We thank CERN for the very successful operation of the LHC, as well as the support staff from our institutions, without whom ATLAS could not be operated efficiently. We acknowledge the support of ANPCyT, Argentina; YerPhI, Armenia; ARC, Australia; BMWFW and FWF, Austria; ANAS, Azerbaijan; SSTC, Belarus; CNPq and FAPESP, Brazil; NSERC, NRC, and CFI, Canada; CERN; CONICYT, Chile; CAS, MOST, and NSFC, China; COLCIENCIAS, Colombia; MSMT CR, MPO CR, and VSC CR, Czech Republic; DNRF, DNSRC, and Lundbeck Foundation, Denmark; EPLANET, ERC, and NSRF, European Union; IN2P3-CNRS, CEA-DSM/IRFU, France; GNSF, Georgia; BMBF, DFG, HGF, MPG, and AvH Foundation, Germany; GSRT and NSRF, Greece; RGC, Hong Kong SAR, China; ISF, MINERVA, GIF, I-CORE, and Benoziyo Center, Israel; INFN, Italy; MEXT and JSPS, Japan; CNRST, Morocco; FOM and NWO, The Netherlands; BRF and RCN, Norway; MNiSW and NCN, Poland; GRICES and FCT, Portugal; MNE/IFA, Romania; MES of Russia and NRC KI, Russian Federation; JINR; MSTD, Serbia; MSSR, Slovakia; ARRS and MIZŠ, Slovenia; DST/NRF, South Africa; MINECO, Spain; SRC and Wallenberg Foundation, Sweden; SER, SNSF, and Cantons of Bern and Geneva, Switzerland; NSC, Taiwan; TAEK, Turkey; STFC, the Royal Society and Leverhulme Trust, United Kingdom; and DOE and NSF, United States of America. The crucial computing support from all WLCG partners is acknowledged gratefully, in particular, from CERN and the ATLAS Tier-1 facilities at TRIUMF (Canada), NDGF (Denmark, Norway, Sweden), CC-IN2P3 (France), KIT/GridKA (Germany), INFN-CNAF (Italy), NL-T1 (The Netherlands), PIC (Spain), ASGC (Taiwan), RAL (UK), and BNL (USA) and in the Tier-2 facilities worldwide.

-
- [1] CMS Collaboration, *Phys. Lett. B* **710**, 256 (2012).
 - [2] CMS Collaboration, *Phys. Lett. B* **715**, 66 (2012).
 - [3] ATLAS Collaboration, *Eur. Phys. J. C* **75**, 23 (2015).
 - [4] ATLAS Collaboration, *Phys. Rev. Lett.* **110**, 022301 (2013).
 - [5] CMS Collaboration, *J. High Energy Phys.* **03** (2015) 022.
 - [6] T. Sjöstrand, S. Mrenna, and P. Z. Skands, *Comput. Phys. Commun.* **178**, 852 (2008).
 - [7] H. Paukkunen, PoS **DIS2014**, 053 (2014).
 - [8] B. Abelev *et al.* (ALICE Collaboration), *Phys. Lett. B* **719**, 29 (2013).
 - [9] CMS Collaboration, *Phys. Lett. B* **718**, 795 (2013).
 - [10] ATLAS Collaboration, *Phys. Rev. Lett.* **110**, 182302 (2013).
 - [11] B. Abelev *et al.* (ALICE Collaboration), *Phys. Lett. B* **726**, 164 (2013).
 - [12] CMS Collaboration, *Phys. Lett. B* **724**, 213 (2013).
 - [13] ATLAS Collaboration, *Phys. Lett. B* **725**, 60 (2013).
 - [14] ATLAS Collaboration, *Phys. Rev. C* **90**, 044906 (2014).
 - [15] ATLAS Collaboration, *Phys. Lett. B* **748**, 392 (2015).
 - [16] CMS Collaboration, *Eur. Phys. J. C* **74**, 2951 (2014).
 - [17] CMS Collaboration, *Phys. Lett. B* **750**, 565 (2015).
 - [18] R. Aaij *et al.* (LHCb Collaboration), *J. High Energy Phys.* **09** (2011) 030.
 - [19] ATLAS Collaboration, *Eur. Phys. J. C* **73**, 2518 (2013).
 - [20] ATLAS Collaboration, *Eur. Phys. J. C* **72**, 1849 (2012).
 - [21] ATLAS Collaboration, *Eur. Phys. J. C* **73**, 1 (2013).
 - [22] ATLAS Collaboration, [arXiv:1508.00848 \[hep-ex\]](https://arxiv.org/abs/1508.00848).
 - [23] ATLAS Collaboration, *Eur. Phys. J. C* **74**, 2941 (2014).
 - [24] ATLAS Collaboration, *Eur. Phys. J. C* **74**, 3130 (2014).
 - [25] M. L. Miller, K. Reygers, S. J. Sanders, and P. Steinberg, *Annu. Rev. Nucl. Part. Sci.* **57**, 205 (2007).
 - [26] V. Guzey and M. Strikman, *Phys. Lett. B* **633**, 245 (2006).
 - [27] M. Alvioli and M. Strikman, *Phys. Lett. B* **722**, 347 (2013).
 - [28] A. Adare *et al.* (PHENIX Collaboration), *Phys. Rev. C* **90**, 034902 (2014).
 - [29] J. Adam *et al.* (ALICE Collaboration), *Phys. Rev. C* **91**, 064905 (2015).

- [30] D. V. Perepelitsa and P. A. Steinberg, arXiv:1412.0976 [nucl-ex].
- [31] S. Alioli, P. Nason, C. Oleari, and E. Re, *J. High Energy Phys.* **07** (2008) 060.
- [32] H.-L. Lai, M. Guzzi, J. Huston, Z. Li, P. M. Nadolsky, J. Pumplin, and C.-P. Yuan, *Phys. Rev. D* **82**, 074024 (2010).
- [33] S. Agostinelli *et al.* (GEANT4 Collaboration), *Nucl. Instrum. Methods A* **506**, 250 (2003).
- [34] ATLAS Collaboration, *Eur. Phys. J. C* **70**, 823 (2010).
- [35] A. Glazov, *AIP Conf. Proc.* **792**, 237 (2005).
- [36] F. Aaron *et al.* (H1 Collaboration), *Eur. Phys. J. C* **63**, 625 (2009).
- [37] R. Gavin, Y. Li, F. Petriello, and S. Quackenbush, *Comput. Phys. Commun.* **182**, 2388 (2011).
- [38] H. Paukkunen and C. A. Salgado, *J. High Energy Phys.* **03** (2011) 071.

-
- G. Aad,⁸⁵ B. Abbott,¹¹³ J. Abdallah,¹⁵¹ O. Abdinov,¹¹ R. Aben,¹⁰⁷ M. Abolins,⁹⁰ O. S. AbouZeid,¹⁵⁸ H. Abramowicz,¹⁵³ H. Abreu,¹⁵² R. Abreu,¹¹⁶ Y. Abulaiti,^{146a,146b} B. S. Acharya,^{164a,164b,a} L. Adamczyk,^{38a} D. L. Adams,²⁵ J. Adelman,¹⁰⁸ S. Adomeit,¹⁰⁰ T. Adye,¹³¹ A. A. Affolder,⁷⁴ T. Agatonovic-Jovin,¹³ J. Agricola,⁵⁴ J. A. Aguilar-Saavedra,^{126a,126f} S. P. Ahlen,²² F. Ahmadov,^{65,b} G. Aielli,^{133a,133b} H. Akerstedt,^{146a,146b} T. P. A. Åkesson,⁸¹ A. V. Akimov,⁹⁶ G. L. Alberghi,^{20a,20b} J. Albert,¹⁶⁹ S. Albrand,⁵⁵ M. J. Alconada Verzini,⁷¹ M. Aleksa,³⁰ I. N. Aleksandrov,⁶⁵ C. Alexa,^{26a} G. Alexander,¹⁵³ T. Alexopoulos,¹⁰ M. Alhroob,¹¹³ G. Alimonti,^{91a} L. Alio,⁸⁵ J. Alison,³¹ S. P. Alkire,³⁵ B. M. M. Allbrooke,¹⁴⁹ P. P. Allport,⁷⁴ A. Aloisio,^{104a,104b} A. Alonso,³⁶ F. Alonso,⁷¹ C. Alpigiani,⁷⁶ A. Altheimer,³⁵ B. Alvarez Gonzalez,³⁰ D. Álvarez Piqueras,¹⁶⁷ M. G. Alviggi,^{104a,104b} B. T. Amadio,¹⁵ K. Amako,⁶⁶ Y. Amaral Coutinho,^{24a} C. Amelung,²³ D. Amidei,⁸⁹ S. P. Amor Dos Santos,^{126a,126c} A. Amorim,^{126a,126b} S. Amoroso,⁴⁸ N. Amram,¹⁵³ G. Amundsen,²³ C. Anastopoulos,¹³⁹ L. S. Ancu,⁴⁹ N. Andari,¹⁰⁸ T. Andeen,³⁵ C. F. Anders,^{58b} G. Anders,³⁰ J. K. Anders,⁷⁴ K. J. Anderson,³¹ A. Andreazza,^{91a,91b} V. Andrei,^{58a} S. Angelidakis,⁹ I. Angelozzi,¹⁰⁷ P. Anger,⁴⁴ A. Angerami,³⁵ F. Anghinolfi,³⁰ A. V. Anisenkov,^{109,c} N. Anjos,¹² A. Annovi,^{124a,124b} M. Antonelli,⁴⁷ A. Antonov,⁹⁸ J. Antos,^{144b} F. Anulli,^{132a} M. Aoki,⁶⁶ L. Aperio Bella,¹⁸ G. Arabidze,⁹⁰ Y. Arai,⁶⁶ J. P. Araque,^{126a} A. T. H. Arce,⁴⁵ F. A. Arduh,⁷¹ J.-F. Arguin,⁹⁵ S. Argyropoulos,⁴² M. Arik,^{19a} A. J. Armbruster,³⁰ O. Arnæz,³⁰ V. Arnal,⁸² H. Arnold,⁴⁸ M. Arratia,²⁸ O. Arslan,²¹ A. Artamonov,⁹⁷ G. Artoni,²³ S. Asai,¹⁵⁵ N. Asbah,⁴² A. Ashkenazi,¹⁵³ B. Åsman,^{146a,146b} L. Asquith,¹⁴⁹ K. Assamagan,²⁵ R. Astalos,^{144a} M. Atkinson,¹⁶⁵ N. B. Atlay,¹⁴¹ K. Augsten,¹²⁸ M. Aurousseau,^{145b} G. Avolio,³⁰ B. Axen,¹⁵ M. K. Ayoub,¹¹⁷ G. Azuelos,^{95,d} M. A. Baak,³⁰ A. E. Baas,^{58a} M. J. Baca,¹⁸ C. Bacci,^{134a,134b} H. Bachacou,¹³⁶ K. Bachas,¹⁵⁴ M. Backes,³⁰ M. Backhaus,³⁰ P. Bagiacchi,^{132a,132b} P. Bagnaia,^{132a,132b} Y. Bai,^{33a} T. Bain,³⁵ J. T. Baines,¹³¹ O. K. Baker,¹⁷⁶ E. M. Baldin,^{109,c} P. Balek,¹²⁹ T. Balestri,¹⁴⁸ F. Balli,⁸⁴ E. Banas,³⁹ Sw. Banerjee,¹⁷³ A. A. E. Bannoura,¹⁷⁵ H. S. Bansil,¹⁸ L. Barak,³⁰ E. L. Barberio,⁸⁸ D. Barberis,^{50a,50b} M. Barbero,⁸⁵ T. Barillari,¹⁰¹ M. Barisonzi,^{164a,164b} T. Barklow,¹⁴³ N. Barlow,²⁸ S. L. Barnes,⁸⁴ B. M. Barnett,¹³¹ R. M. Barnett,¹⁵ Z. Barnovska,⁵ A. Baroncelli,^{134a} G. Barone,²³ A. J. Barr,¹²⁰ F. Barreiro,⁸² J. Barreiro Guimarães da Costa,⁵⁷ R. Bartoldus,¹⁴³ A. E. Barton,⁷² P. Bartos,^{144a} A. Basalaev,¹²³ A. Bassalat,¹¹⁷ A. Basye,¹⁶⁵ R. L. Bates,⁵³ S. J. Batista,¹⁵⁸ J. R. Batley,²⁸ M. Battaglia,¹³⁷ M. Bauce,^{132a,132b} F. Bauer,¹³⁶ H. S. Bawa,^{143,e} J. B. Beacham,¹¹¹ M. D. Beattie,⁷² T. Beau,⁸⁰ P. H. Beauchemin,¹⁶¹ R. Beccherle,^{124a,124b} P. Bechtle,²¹ H. P. Beck,^{17,f} K. Becker,¹²⁰ M. Becker,⁸³ S. Becker,¹⁰⁰ M. Beckingham,¹⁷⁰ C. Becot,¹¹⁷ A. J. Beddall,^{19b} A. Beddall,^{19b} V. A. Bednyakov,⁶⁵ C. P. Bee,¹⁴⁸ L. J. Beemster,¹⁰⁷ T. A. Beermann,¹⁷⁵ M. Begel,²⁵ J. K. Behr,¹²⁰ C. Belanger-Champagne,⁸⁷ W. H. Bell,⁴⁹ G. Bella,¹⁵³ L. Bellagamba,^{20a} A. Bellerive,²⁹ M. Bellomo,⁸⁶ K. Belotskiy,⁹⁸ O. Beltramello,³⁰ O. Benary,¹⁵³ D. Benchekroun,^{135a} M. Bender,¹⁰⁰ K. Bendtz,^{146a,146b} N. Benekos,¹⁰ Y. Benhammou,¹⁵³ E. Benhar Noccioli,⁴⁹ J. A. Benitez Garcia,^{159b} D. P. Benjamin,⁴⁵ J. R. Bensinger,²³ S. Bentvelsen,¹⁰⁷ L. Beresford,¹²⁰ M. Beretta,⁴⁷ D. Berge,¹⁰⁷ E. Bergeaas Kuutmann,¹⁶⁶ N. Berger,⁵ F. Berghaus,¹⁶⁹ J. Beringer,¹⁵ C. Bernard,²² N. R. Bernard,⁸⁶ C. Bernius,¹¹⁰ F. U. Bernlochner,²¹ T. Berry,⁷⁷ P. Berta,¹²⁹ C. Bertella,⁸³ G. Bertoli,^{146a,146b} F. Bertolucci,^{124a,124b} C. Bertsche,¹¹³ D. Bertsche,¹¹³ M. I. Besana,^{91a} G. J. Besjes,³⁶ O. Bessidskaia Bylund,^{146a,146b} M. Bessner,⁴² N. Besson,¹³⁶ C. Betancourt,⁴⁸ S. Bethke,¹⁰¹ A. J. Bevan,⁷⁶ W. Bhimji,¹⁵ R. M. Bianchi,¹²⁵ L. Bianchini,²³ M. Bianco,³⁰ O. Biebel,¹⁰⁰ D. Biedermann,¹⁶ S. P. Bieniek,⁷⁸ M. Biglietti,^{134a} J. Bilbao De Mendizabal,⁴⁹ H. Bilokon,⁴⁷ M. Bindi,⁵⁴ S. Binet,¹¹⁷ A. Bingul,^{19b} C. Bini,^{132a,132b} S. Biondi,^{20a,20b} C. W. Black,¹⁵⁰ J. E. Black,¹⁴³ K. M. Black,²² D. Blackburn,¹³⁸ R. E. Blair,⁶ J.-B. Blanchard,¹³⁶ J. E. Blanco,⁷⁷ T. Blazek,^{144a} I. Bloch,⁴² C. Blocker,²³ W. Blum,^{83,*} U. Blumenschein,⁵⁴ G. J. Bobbink,¹⁰⁷ V. S. Bobrovnikov,^{109,c} S. S. Bocchetta,⁸¹ A. Bocci,⁴⁵ C. Bock,¹⁰⁰ M. Boehler,⁴⁸ J. A. Bogaerts,³⁰ D. Bogavac,¹³ A. G. Bogdanchikov,¹⁰⁹ C. Bohm,^{146a} V. Boisvert,⁷⁷ T. Bold,^{38a} V. Boldea,^{26a} A. S. Boldyrev,⁹⁹ M. Bomben,⁸⁰ M. Bona,⁷⁶ M. Boonekamp,¹³⁶ A. Borisov,¹³⁰ G. Borissov,⁷² S. Borroni,⁴² J. Bortfeldt,¹⁰⁰ V. Bortolotto,^{60a,60b,60c} K. Bos,¹⁰⁷ D. Boscherini,^{20a} M. Bosman,¹² J. Boudreau,¹²⁵ J. Bouffard,² E. V. Bouhova-Thacker,⁷² D. Boumediene,³⁴ C. Bourdarios,¹¹⁷ N. Bousson,¹¹⁴ A. Boveia,³⁰ J. Boyd,³⁰ I. R. Boyko,⁶⁵ I. Bozic,¹³ J. Bracinik,¹⁸ A. Brandt,⁸ G. Brandt,⁵⁴ O. Brandt,^{58a} U. Bratzler,¹⁵⁶ B. Brau,⁸⁶ J. E. Brau,¹¹⁶ H. M. Braun,^{175,*} S. F. Brazzale,^{164a,164c} W. D. Breaden Madden,⁵³ K. Brendlinger,¹²² A. J. Brennan,⁸⁸ L. Brenner,¹⁰⁷ R. Brenner,¹⁶⁶ S. Bressler,¹⁷² K. Bristow,^{145c} T. M. Bristow,⁴⁶ D. Britton,⁵³ D. Britzger,⁴² F. M. Brochu,²⁸ I. Brock,²¹ R. Brock,⁹⁰ J. Bronner,¹⁰¹ G. Brooijmans,³⁵ T. Brooks,⁷⁷ W. K. Brooks,^{32b} J. Brosamer,¹⁵ E. Brost,¹¹⁶ J. Brown,⁵⁵ P. A. Bruckman de Renstrom,³⁹ D. Bruncko,^{144b} R. Bruneliere,⁴⁸ A. Bruni,^{20a} G. Bruni,^{20a} M. Bruschi,^{20a} N. Bruscino,²¹ L. Bryngemark,⁸¹ T. Buanes,¹⁴ Q. Buat,¹⁴² P. Buchholz,¹⁴¹ A. G. Buckley,⁵³ S. I. Buda,^{26a} I. A. Budagov,⁶⁵ F. Buehrer,⁴⁸ L. Bugge,¹¹⁹

- M. K. Bugge,¹¹⁹ O. Bulekov,⁹⁸ D. Bullock,⁸ H. Burckhart,³⁰ S. Burdin,⁷⁴ B. Burghgrave,¹⁰⁸ S. Burke,¹³¹ I. Burmeister,⁴³
 E. Busato,³⁴ D. Büscher,⁴⁸ V. Büscher,⁸³ P. Bussey,⁵³ J. M. Butler,²² A. I. Butt,³ C. M. Buttar,⁵³ J. M. Butterworth,⁷⁸ P. Butt,¹⁰⁷
 W. Buttinger,²⁵ A. Buzatu,⁵³ A. R. Buzykaev,^{109,c} S. Cabrera Urbán,¹⁶⁷ D. Caforio,¹²⁸ V. M. Cairo,^{37a,37b} O. Cakir,^{4a}
 N. Calace,⁴⁹ P. Calafiura,¹⁵ A. Calandri,¹³⁶ G. Calderini,⁸⁰ P. Calfayan,¹⁰⁰ L. P. Caloba,^{24a} D. Calvet,³⁴ S. Calvet,³⁴
 R. Camacho Toro,³¹ S. Camarda,⁴² P. Camarri,^{133a,133b} D. Cameron,¹¹⁹ R. Caminal Armadans,¹⁶⁵ S. Campana,³⁰
 M. Campanelli,⁷⁸ A. Campoverde,¹⁴⁸ V. Canale,^{104a,104b} A. Canepa,^{159a} M. Cano Bret,^{33e} J. Cantero,⁸² R. Cantrill,^{126a} T. Cao,⁴⁰
 M. D. M. Capeans Garrido,³⁰ I. Caprini,^{26a} M. Caprini,^{26a} M. Capua,^{37a,37b} R. Caputo,⁸³ R. Cardarelli,^{133a} F. Cardillo,⁴⁸
 T. Carli,³⁰ G. Carlino,^{104a} L. Carminati,^{91a,91b} S. Caron,¹⁰⁶ E. Carquin,^{32a} G. D. Carrillo-Montoya,⁸ J. R. Carter,²⁸
 J. Carvalho,^{126a,126c} D. Casadei,⁷⁸ M. P. Casado,¹² M. Casolino,¹² E. Castaneda-Miranda,^{145b} A. Castelli,¹⁰⁷
 V. Castillo Gimenez,¹⁶⁷ N. F. Castro,^{126a,g} P. Catastini,⁵⁷ A. Catinaccio,³⁰ J. R. Catmore,¹¹⁹ A. Cattai,³⁰ J. Caudron,⁸³
 V. Cavaliere,¹⁶⁵ D. Cavalli,^{91a} M. Cavalli-Sforza,¹² V. Cavasinni,^{124a,124b} F. Ceradini,^{134a,134b} B. C. Cerio,⁴⁵ K. Cerny,¹²⁹
 A. S. Cerqueira,^{24b} A. Cerri,¹⁴⁹ L. Cerrito,⁷⁶ F. Cerutti,¹⁵ M. Cerv,³⁰ A. Cervelli,¹⁷ S. A. Cetin,^{19c} A. Chafaq,^{135a}
 D. Chakraborty,¹⁰⁸ I. Chalupkova,¹²⁹ P. Chang,¹⁶⁵ J. D. Chapman,²⁸ D. G. Charlton,¹⁸ C. C. Chau,¹⁵⁸ C. A. Chavez Barajas,¹⁴⁹
 S. Cheatham,¹⁵² A. Chegwidden,⁹⁰ S. Chekanov,⁶ S. V. Chekulaev,^{159a} G. A. Chelkov,^{65,h} M. A. Chelstowska,⁸⁹ C. Chen,⁶⁴
 H. Chen,²⁵ K. Chen,¹⁴⁸ L. Chen,^{33d,i} S. Chen,^{33c} X. Chen,^{33f} Y. Chen,⁶⁷ H. C. Cheng,⁸⁹ Y. Cheng,³¹ A. Cheplakov,⁶⁵
 E. Cheremushkina,¹³⁰ R. Cherkaoui El Moursli,^{135e} V. Chernyatin,^{25,*} E. Cheu,⁷ L. Chevalier,¹³⁶ V. Chiarella,⁴⁷
 G. Chiarelli,^{124a,124b} J. T. Childers,⁶ G. Chiodini,^{73a} A. S. Chisholm,¹⁸ R. T. Chislett,⁷⁸ A. Chitan,^{26a} M. V. Chizhov,⁶⁵
 K. Choi,⁶¹ S. Chouridou,⁹ B. K. B. Chow,¹⁰⁰ V. Christodoulou,⁷⁸ D. Chromek-Burckhart,³⁰ J. Chudoba,¹²⁷ A. J. Chuinard,⁸⁷
 J. J. Chwastowski,³⁹ L. Chytka,¹¹⁵ G. Ciapetti,^{132a,132b} A. K. Ciftci,^{4a} D. Cinca,⁵³ V. Cindro,⁷⁵ I. A. Cioara,²¹ A. Ciocio,¹⁵
 Z. H. Citron,¹⁷² M. Ciubancan,^{26a} A. Clark,⁴⁹ B. L. Clark,⁵⁷ P. J. Clark,⁴⁶ R. N. Clarke,¹⁵ W. Cleland,¹²⁵ C. Clement,^{146a,146b}
 Y. Coadou,⁸⁵ M. Cobal,^{164a,164c} A. Coccaro,¹³⁸ J. Cochran,⁶⁴ L. Coffey,²³ J. G. Cogan,¹⁴³ L. Colasurdo,¹⁰⁶ B. Cole,³⁵ S. Cole,¹⁰⁸
 A. P. Colijn,¹⁰⁷ J. Collot,⁵⁵ T. Colombo,^{58c} G. Compostella,¹⁰¹ P. Conde Muiño,^{126a,126b} E. Coniavitis,⁴⁸ S. H. Connell,^{145b}
 I. A. Connelly,⁷⁷ S. M. Consonni,^{91a,91b} V. Consorti,⁴⁸ S. Constantinescu,^{26a} C. Conta,^{121a,121b} G. Conti,³⁰ F. Conventi,^{104a,j}
 M. Cooke,¹⁵ B. D. Cooper,⁷⁸ A. M. Cooper-Sarkar,¹²⁰ T. Cornelissen,¹⁷⁵ M. Corradi,^{20a} F. Corriveau,^{87,k} A. Corso-Radu,¹⁶³
 A. Cortes-Gonzalez,¹² G. Cortiana,¹⁰¹ G. Costa,^{91a} M. J. Costa,¹⁶⁷ D. Costanzo,¹³⁹ D. Côté,⁸ G. Cottin,²⁸ G. Cowan,⁷⁷
 B. E. Cox,⁸⁴ K. Cranmer,¹¹⁰ G. Cree,²⁹ S. Crépé-Renaudin,⁵⁵ F. Crescioli,⁸⁰ W. A. Cribbs,^{146a,146b} M. Crispin Ortizar,¹²⁰
 M. Cristinziani,²¹ V. Croft,¹⁰⁶ G. Crosetti,^{37a,37b} T. Cuhadar Donszelmann,¹³⁹ J. Cummings,¹⁷⁶ M. Curatolo,⁴⁷ C. Cuthbert,¹⁵⁰
 H. Czirr,¹⁴¹ P. Czodrowski,³ S. D'Auria,⁵³ M. D'Onofrio,⁷⁴ M. J. Da Cunha Sargedas De Sousa,^{126a,126b} C. Da Via,⁸⁴
 W. Dabrowski,^{38a} A. Dafinca,¹²⁰ T. Dai,⁸⁹ O. Dale,¹⁴ F. Dallaire,⁹⁵ C. Dallapiccola,⁸⁶ M. Dam,³⁶ J. R. Dandoy,³¹ N. P. Dang,⁴⁸
 A. C. Daniells,¹⁸ M. Danninger,¹⁶⁸ M. Dano Hoffmann,¹³⁶ V. Dao,⁴⁸ G. Darbo,^{50a} S. Darmora,⁸ J. Dassoulas,³ A. Dattagupta,⁶¹
 W. Davey,²¹ C. David,¹⁶⁹ T. Davidek,¹²⁹ E. Davies,^{120,i} M. Davies,¹⁵³ P. Davison,⁷⁸ Y. Davygora,^{58a} E. Dawe,⁸⁸ I. Dawson,¹³⁹
 R. K. Daya-Ishmukhametova,⁸⁶ K. De,⁸ R. de Asmundis,^{104a} A. De Benedetti,¹¹³ S. De Castro,^{20a,20b} S. De Cecco,⁸⁰
 N. De Groot,¹⁰⁶ P. de Jong,¹⁰⁷ H. De la Torre,⁸² F. De Lorenzi,⁶⁴ L. De Nooij,¹⁰⁷ D. De Pedis,^{132a} A. De Salvo,^{132a}
 U. De Sanctis,¹⁴⁹ A. De Santo,¹⁴⁹ J. B. De Vivie De Regie,¹¹⁷ W. J. Dearnaley,⁷² R. Debbe,²⁵ C. Debenedetti,¹³⁷
 D. V. Dedovich,⁶⁵ I. Deigaard,¹⁰⁷ J. Del Peso,⁸² T. Del Prete,^{124a,124b} D. Delgove,¹¹⁷ F. Deliot,¹³⁶ C. M. Delitzsch,⁴⁹
 M. Deliyergiyev,⁷⁵ A. Dell'Acqua,³⁰ L. Dell'Asta,²² M. Dell'Orso,^{124a,124b} M. Della Pietra,^{104a,j} D. della Volpe,⁴⁹
 M. Delmastro,⁵ P. A. Delsart,⁵⁵ C. Deluca,¹⁰⁷ D. A. DeMarco,¹⁵⁸ S. Demers,¹⁷⁶ M. Demichev,⁶⁵ A. Demilly,⁸⁰ S. P. Denisov,¹³⁰
 D. Derendarz,³⁹ J. E. Derkaoui,^{135d} F. Derue,⁸⁰ P. Dervan,⁷⁴ K. Desch,²¹ C. Deterre,⁴² P. O. Deviveiros,³⁰ A. Dewhurst,¹³¹
 S. Dhaliwal,²³ A. Di Ciaccio,^{133a,133b} L. Di Ciaccio,⁵ A. Di Domenico,^{132a,132b} C. Di Donato,^{104a,104b} A. Di Girolamo,³⁰
 B. Di Girolamo,³⁰ A. Di Mattia,¹⁵² B. Di Micco,^{134a,134b} R. Di Nardo,⁴⁷ A. Di Simone,⁴⁸ R. Di Sipio,¹⁵⁸ D. Di Valentino,²⁹
 C. Diaconu,⁸⁵ M. Diamond,¹⁵⁸ F. A. Dias,⁴⁶ M. A. Diaz,^{32a} E. B. Diehl,⁸⁹ J. Dietrich,¹⁶ S. Diglio,⁸⁵ A. Dimitrijevska,¹³
 J. Dingfelder,²¹ P. Dita,^{26a} S. Dita,^{26a} F. Dittus,³⁰ F. Djama,⁸⁵ T. Djobava,^{51b} J. I. Djuvsland,^{58a} M. A. B. do Vale,^{24c} D. Dobos,³⁰
 M. Dobre,^{26a} C. Doglioni,⁸¹ T. Dohmae,¹⁵⁵ J. Dolejsi,¹²⁹ Z. Dolezal,¹²⁹ B. A. Dolgoshein,^{98,*} M. Donadelli,^{24d}
 S. Donati,^{124a,124b} P. Dondero,^{121a,121b} J. Donini,³⁴ J. Dopke,¹³¹ A. Doria,^{104a} M. T. Dova,⁷¹ A. T. Doyle,⁵³ E. Drechsler,⁵⁴
 M. Dris,¹⁰ E. Dubreuil,¹⁷² E. Duchovni,¹⁷² G. Duckeck,¹⁰⁰ O. A. Ducu,^{26a,85} D. Duda,¹⁰⁷ A. Dudarev,³⁰ L. Duflot,¹¹⁷
 L. Duguid,⁷⁷ M. Dührssen,³⁰ M. Dunford,^{58a} H. Duran Yildiz,^{4a} M. Düren,⁵² A. Durglishvili,^{51b} D. Duschinger,⁴⁴ M. Dyndal,^{38a}
 C. Eckhardt,⁴² K. M. Ecker,¹⁰¹ R. C. Edgar,⁸⁹ W. Edson,² N. C. Edwards,⁴⁶ W. Ehrenfeld,²¹ T. Eifert,³⁰ G. Eigen,¹⁴
 K. Einsweiler,¹⁵ T. Ekelof,¹⁶⁶ M. El Kacimi,^{135c} M. Ellert,¹⁶⁶ S. Elles,⁵ F. Ellinghaus,¹⁷⁵ A. A. Elliot,¹⁶⁹ N. Ellis,³⁰
 J. Elmsheuser,¹⁰⁰ M. Elsing,³⁰ D. Emeliyanov,¹³¹ Y. Enari,¹⁵⁵ O. C. Endner,⁸³ M. Endo,¹¹⁸ J. Erdmann,⁴³ A. Ereditato,¹⁷
 G. Ernis,¹⁷⁵ J. Ernst,² M. Ernst,²⁵ S. Errede,¹⁶⁵ E. Ertel,⁸³ M. Escalier,¹¹⁷ H. Esch,⁴³ C. Escobar,¹²⁵ B. Esposito,⁴⁷
 A. I. Etienne,¹³⁶ E. Etzion,¹⁵³ H. Evans,⁶¹ A. Ezhilov,¹²³ L. Fabbri,^{20a,20b} G. Facini,³¹ R. M. Fakhruddinov,¹³⁰ S. Falciano,^{132a}
 R. J. Falla,⁷⁸ J. Faltova,¹²⁹ Y. Fang,^{33a} M. Fanti,^{91a,91b} A. Farbin,⁸ A. Farilla,^{134a} T. Farooque,¹² S. Farrell,¹⁵ S. M. Farrington,¹⁷⁰
 P. Farthouat,³⁰ F. Fassi,^{135e} P. Fassnacht,³⁰ D. Fassouliotis,⁹ M. Faucci Giannelli,⁷⁷ A. Favareto,^{50a,50b} L. Fayard,¹¹⁷
 P. Federic,^{144a} O. L. Fedin,^{123,m} W. Fedorko,¹⁶⁸ S. Feigl,³⁰ L. Feligioni,⁸⁵ C. Feng,^{33d} E. J. Feng,⁶ H. Feng,⁸⁹ A. B. Fenyuk,¹³⁰
 L. Feremenga,⁸ P. Fernandez Martinez,¹⁶⁷ S. Fernandez Perez,³⁰ J. Ferrando,⁵³ A. Ferrari,¹⁶⁶ P. Ferrari,¹⁰⁷ R. Ferrari,^{121a}
 D. E. Ferreira de Lima,⁵³ A. Ferrer,¹⁶⁷ D. Ferrere,⁴⁹ C. Ferretti,⁸⁹ A. Ferretto Parodi,^{50a,50b} M. Fiascaris,³¹ F. Fiedler,⁸³
 A. Filipčić,⁷⁵ M. Filizzuzzi,⁴² F. Filthaut,¹⁰⁶ M. Fincke-Keeler,¹⁶⁹ K. D. Finelli,¹⁵⁰ M. C. N. Fiolhais,^{126a,126c} L. Fiorini,¹⁶⁷
 A. Firat,⁴⁰ A. Fischer,² C. Fischer,¹² J. Fischer,¹⁷⁵ W. C. Fisher,⁹⁰ E. A. Fitzgerald,²³ N. Flaschel,⁴² I. Fleck,¹⁴¹

- P. Fleischmann,⁸⁹ S. Fleischmann,¹⁷⁵ G. T. Fletcher,¹³⁹ G. Fletcher,⁷⁶ R. R. M. Fletcher,¹²² T. Flick,¹⁷⁵ A. Floderus,⁸¹
L. R. Flores Castillo,^{60a} M. J. Flowerdew,¹⁰¹ A. Formica,¹³⁶ A. Forti,⁸⁴ D. Fournier,¹¹⁷ H. Fox,⁷² S. Fracchia,¹² P. Francavilla,⁸⁰
M. Franchini,^{20a,20b} D. Francis,³⁰ L. Franconi,¹¹⁹ M. Franklin,⁵⁷ M. Frate,¹⁶³ M. Fraternali,^{121a,121b} D. Freeborn,⁷⁸
S. T. French,²⁸ F. Friedrich,⁴⁴ D. Froidevaux,³⁰ J. A. Frost,¹²⁰ C. Fukunaga,¹⁵⁶ E. Fullana Torregrosa,⁸³ B. G. Fulsom,¹⁴³
T. Fusayasu,¹⁰² J. Fuster,¹⁶⁷ C. Gabaldon,⁵⁵ O. Gabizon,¹⁷⁵ A. Gabrielli,^{20a,20b} A. Gabrielli,^{132a,132b} G. P. Gach,^{38a}
S. Gadatsch,¹⁰⁷ S. Gadomski,⁴⁹ G. Gagliardi,^{50a,50b} P. Gagnon,⁶¹ C. Galea,¹⁰⁶ B. Galhardo,^{126a,126c} E. J. Gallas,¹²⁰
B. J. Gallop,¹³¹ P. Gallus,¹²⁸ G. Galster,³⁶ K. K. Gan,¹¹¹ J. Gao,^{33b,85} Y. Gao,⁴⁶ Y. S. Gao,^{143,e} F. M. Garay Walls,⁴⁶
F. Garberson,¹⁷⁶ C. García,¹⁶⁷ J. E. García Navarro,¹⁶⁷ M. Garcia-Sciveres,¹⁵ R. W. Gardner,³¹ N. Garelli,¹⁴³ V. Garonne,¹¹⁹
C. Gatti,⁴⁷ A. Gaudiello,^{50a,50b} G. Gaudio,^{121a} B. Gaur,¹⁴¹ L. Gauthier,⁹⁵ P. Gauzzi,^{132a,132b} I. L. Gavrilenko,⁹⁶ C. Gay,¹⁶⁸
G. Gaycken,²¹ E. N. Gazis,¹⁰ P. Ge,^{33d} Z. Gecse,¹⁶⁸ C. N. P. Gee,¹³¹ D. A. A. Geerts,¹⁰⁷ Ch. Geich-Gimbel,²¹ M. P. Geisler,^{58a}
C. Gemme,^{50a} M. H. Genest,⁵⁵ S. Gentile,^{132a,132b} M. George,⁵⁴ S. George,⁷⁷ D. Gerbaudo,¹⁶³ A. Gershon,¹⁵³ S. Ghasemi,¹⁴¹
H. Ghazlane,^{135b} B. Giacobbe,^{20a} S. Giagu,^{132a,132b} V. Giangiobbe,¹² P. Giannetti,^{124a,124b} B. Gibbard,²⁵ S. M. Gibson,⁷⁷
M. Gilchriese,¹⁵ T. P. S. Gillam,²⁸ D. Gillberg,³⁰ G. Gilles,³⁴ D. M. Gingrich,^{3,d} N. Giokaris,⁹ M. P. Giordani,^{164a,164c}
F. M. Giorgi,^{20a} F. M. Giorgi,¹⁶ P. F. Giraud,¹³⁶ P. Giromini,⁴⁷ D. Giugni,^{91a} C. Giuliani,⁴⁸ M. Giulini,^{58b} B. K. Gjelsten,¹¹⁹
S. Gkaitatzis,¹⁵⁴ I. Gkalias,¹⁵⁴ E. L. Gkougkousis,¹¹⁷ L. K. Gladilin,⁹⁹ C. Glasman,⁸² J. Glatzer,³⁰ P. C. F. Glaysher,⁴⁶
A. Glazov,⁴² M. Goblirsch-Kolb,¹⁰¹ J. R. Goddard,⁷⁶ J. Godlewski,³⁹ S. Goldfarb,⁸⁹ T. Golling,⁴⁹ D. Golubkov,¹³⁰
A. Gomes,^{126a,126b,126d} R. Gonçalo,^{126a} J. Goncalves Pinto Firmino Da Costa,¹³⁶ L. Gonella,²¹ S. González de la Hoz,¹⁶⁷
G. Gonzalez Parra,¹² S. Gonzalez-Sevilla,⁴⁹ L. Goossens,³⁰ P. A. Gorbounov,⁹⁷ H. A. Gordon,²⁵ I. Gorelov,¹⁰⁵ B. Gorini,³⁰
E. Gorini,^{73a,73b} A. Gorišek,⁷⁵ E. Gornicki,³⁹ A. T. Goshaw,⁴⁵ C. Gössling,⁴³ M. I. Gostkin,⁶⁵ D. Goujdami,^{135c}
A. G. Goussiou,¹³⁸ N. Govender,^{145b} E. Gozani,¹⁵² H. M. X. Grabas,¹³⁷ L. Graber,⁵⁴ I. Grabowska-Bold,^{38a} P. O. J. Gradin,¹⁶⁶
P. Grafström,^{20a,20b} K.-J. Grahn,⁴² J. Gramling,⁴⁹ E. Gramstad,¹¹⁹ S. Grancagnolo,¹⁶ V. Grassi,¹⁴⁸ V. Gratchev,¹²³ H. M. Gray,³⁰
E. Graziani,^{134a} Z. D. Greenwood,^{79,n} K. Gregersen,⁷⁸ I. M. Gregor,⁴² P. Grenier,¹⁴³ J. Griffiths,⁸ A. A. Grillo,¹³⁷ K. Grimm,⁷²
S. Grinstein,^{12,o} Ph. Gris,³⁴ J.-F. Grivaz,¹¹⁷ J. P. Grohs,⁴⁴ A. Grohsjean,⁴² E. Gross,¹⁷² J. Grosse-Knetter,⁵⁴ G. C. Grossi,⁷⁹
Z. J. Grout,¹⁴⁹ L. Guan,⁸⁹ J. Guenther,¹²⁸ F. Guescini,⁴⁹ D. Guest,¹⁷⁶ O. Gueta,¹⁵³ E. Guido,^{50a,50b} T. Guillemin,¹¹⁷ S. Guindon,²
U. Gul,⁵³ C. Gumpert,⁴⁴ J. Guo,^{33e} Y. Guo,^{33b} S. Gupta,¹²⁰ G. Gustavino,^{132a,132b} P. Gutierrez,¹¹³ N. G. Gutierrez Ortiz,⁷⁸
C. Gutschow,⁴⁴ C. Guyot,¹³⁶ C. Gwenlan,¹²⁰ C. B. Gwilliam,⁷⁴ A. Haas,¹¹⁰ C. Haber,¹⁵ H. K. Hadavand,⁸ N. Haddad,^{135e}
P. Haefner,²¹ S. Hageböck,²¹ Z. Hajduk,³⁹ H. Hakobyan,¹⁷⁷ M. Haleem,⁴² J. Haley,¹¹⁴ D. Hall,¹²⁰ G. Halladjian,⁹⁰
G. D. Hallewell,⁸⁵ K. Hamacher,¹⁷⁵ P. Hamal,¹¹⁵ K. Hamano,¹⁶⁹ M. Hamer,⁵⁴ A. Hamilton,^{145a} G. N. Hamity,^{145c}
P. G. Hamnett,⁴² L. Han,^{33b} K. Hanagaki,⁶⁶ K. Hanawa,¹⁵⁵ M. Hance,¹⁵ P. Hanke,^{58a} R. Hanna,¹³⁶ J. B. Hansen,³⁶
J. D. Hansen,³⁶ M. C. Hansen,²¹ P. H. Hansen,³⁶ K. Hara,¹⁶⁰ A. S. Hard,¹⁷³ T. Harenberg,¹⁷⁵ F. Hariri,¹¹⁷ S. Harkusha,⁹²
R. D. Harrington,⁴⁶ P. F. Harrison,¹⁷⁰ F. Hartjes,¹⁰⁷ M. Hasegawa,⁶⁷ S. Hasegawa,¹⁰³ Y. Hasegawa,¹⁴⁰ A. Hasib,¹¹³
S. Hassani,¹³⁶ S. Haug,¹⁷ R. Hauser,⁹⁰ L. Hauswald,⁴⁴ M. Havranek,¹²⁷ C. M. Hawkes,¹⁸ R. J. Hawkings,³⁰ A. D. Hawkins,⁸¹
T. Hayashi,¹⁶⁰ D. Hayden,⁹⁰ C. P. Hays,¹²⁰ J. M. Hays,⁷⁶ H. S. Hayward,⁷⁴ S. J. Haywood,¹³¹ S. J. Head,¹⁸ T. Heck,⁸³
V. Hedberg,⁸¹ L. Heelan,⁸ S. Heim,¹²² T. Heim,¹⁷⁵ B. Heinemann,¹⁵ L. Heinrich,¹¹⁰ J. Hejbal,¹²⁷ L. Helary,²²
S. Hellman,^{146a,146b} D. Hellmich,²¹ C. Helsens,¹² J. Henderson,¹²⁰ R. C. W. Henderson,⁷² Y. Heng,¹⁷³ C. Hengler,⁴²
A. Henrichs,¹⁷⁶ A. M. Henriques Correia,³⁰ S. Henrot-Versille,¹¹⁷ G. H. Herbert,¹⁶ Y. Hernández Jiménez,¹⁶⁷
R. Herrberg-Schubert,¹⁶ G. Herten,⁴⁸ R. Hertenberger,¹⁰⁰ L. Hervas,³⁰ G. G. Hesketh,⁷⁸ N. P. Hessey,¹⁰⁷ J. W. Hetherly,⁴⁰
R. Hickling,⁷⁶ E. Higón-Rodríguez,¹⁶⁷ E. Hill,¹⁶⁹ J. C. Hill,²⁸ K. H. Hiller,⁴² S. J. Hillier,¹⁸ I. Hinchliffe,¹⁵ E. Hines,¹²²
R. R. Hinman,¹⁵ M. Hirose,¹⁵⁷ D. Hirschbuehl,¹⁷⁵ J. Hobbs,¹⁴⁸ N. Hod,¹⁰⁷ M. C. Hodgkinson,¹³⁹ P. Hodgson,¹³⁹ A. Hoecker,³⁰
M. R. Hoeferkamp,¹⁰⁵ F. Hoenig,¹⁰⁰ M. Hohlfeld,⁸³ D. Hohn,²¹ T. R. Holmes,¹⁵ M. Homann,⁴³ T. M. Hong,¹²⁵ L. Hooft van
Huysduyven,¹¹⁰ W. H. Hopkins,¹¹⁶ Y. Horii,¹⁰³ A. J. Horton,¹⁴² J.-Y. Hostachy,⁵⁵ S. Hou,¹⁵¹ A. Hoummada,^{135a} J. Howard,¹²⁰
J. Howarth,⁴² M. Hrabovsky,¹¹⁵ I. Hristova,¹⁶ J. Hrivnac,¹¹⁷ T. Hrynevich,⁵ A. Hrynevich,⁹³ C. Hsu,^{145c} P. J. Hsu,^{151,p}
S.-C. Hsu,¹³⁸ D. Hu,³⁵ Q. Hu,^{33b} X. Hu,⁸⁹ Y. Huang,⁴² Z. Hubacek,¹²⁸ F. Hubaut,⁸⁵ F. Huegging,²¹ T. B. Huffman,¹²⁰
E. W. Hughes,³⁵ G. Hughes,⁷² M. Huhtinen,³⁰ T. A. Hülsing,⁸³ N. Huseynov,^{65,b} J. Huston,⁹⁰ J. Huth,⁵⁷ G. Iacobucci,⁴⁹
G. Iakovidis,²⁵ I. Ibragimov,¹⁴¹ L. Iconomidou-Fayard,¹¹⁷ E. Ideal,¹⁷⁶ Z. Idrissi,^{135e} P. Iengo,³⁰ O. Igonkina,¹⁰⁷ T. Iizawa,¹⁷¹
Y. Ikegami,⁶⁶ K. Ikematsu,¹⁴¹ M. Ikeno,⁶⁶ Y. Ilchenko,^{31,q} D. Iliadis,¹⁵⁴ N. Ilic,¹⁴³ T. Ince,¹⁰¹ G. Introzzi,^{121a,121b} P. Ioannou,⁹
M. Iodice,^{134a} K. Iordanidou,³⁵ V. Ippolito,⁵⁷ A. Irles Quiles,¹⁶⁷ C. Isaksson,¹⁶⁶ M. Ishino,⁶⁸ M. Ishitsuka,¹⁵⁷
R. Ishmukhametov,¹¹¹ C. Issever,¹²⁰ S. Istin,^{19a} J. M. Iturbe Ponce,⁸⁴ R. Iuppa,^{133a,133b} J. Ivarsson,⁸¹ W. Iwanski,³⁹
H. Iwasaki,⁶⁶ J. M. Izen,⁴¹ V. Izzo,^{104a} S. Jabbar,³ B. Jackson,¹²² M. Jackson,⁷⁴ P. Jackson,¹ M. R. Jaekel,³⁰ V. Jain,²
K. Jakobs,⁴⁸ S. Jakobsen,³⁰ T. Jakoubek,¹²⁷ J. Jakubek,¹²⁸ D. O. Jamin,¹¹⁴ D. K. Jana,⁷⁹ E. Jansen,⁷⁸ R. Jansky,⁶² J. Janssen,²¹
M. Janus,¹⁷⁰ G. Jarlskog,⁸¹ N. Javadov,^{65,b} T. Javůrek,⁴⁸ L. Jeanty,¹⁵ J. Jejelava,^{51a,r} G.-Y. Jeng,¹⁵⁰ D. Jennens,⁸⁸ P. Jenni,^{48,s}
J. Jentzsch,⁴³ C. Jeske,¹⁷⁰ S. Jézéquel,⁵ H. Ji,¹⁷³ J. Jia,¹⁴⁸ Y. Jiang,^{33b} S. Jiggins,⁷⁸ J. Jimenez Pena,¹⁶⁷ S. Jin,^{33a} A. Jinaru,^{26a}
O. Jinnouchi,¹⁵⁷ M. D. Joergensen,³⁶ P. Johansson,¹³⁹ K. A. Johns,⁷ K. Jon-And,^{146a,146b} G. Jones,¹⁷⁰ R. W. L. Jones,⁷²
T. J. Jones,⁷⁴ J. Jongmanns,^{58a} P. M. Jorge,^{126a,126b} K. D. Joshi,⁸⁴ J. Jovicevic,^{159a} X. Ju,¹⁷³ C. A. Jung,⁴³ P. Jussel,⁶²
A. Juste Rozas,^{12,o} M. Kaci,¹⁶⁷ A. Kaczmar ska,³⁹ M. Kado,¹¹⁷ H. Kagan,¹¹¹ M. Kagan,¹⁴³ S. J. Kahn,⁸⁵ E. Kajomovitz,⁴⁵
C. W. Kalderon,¹²⁰ S. Kama,⁴⁰ A. Kamenshchikov,¹³⁰ N. Kanaya,¹⁵⁵ S. Kaneti,²⁸ V. A. Kantserov,⁹⁸ J. Kanzaki,⁶⁶ B. Kaplan,¹¹⁰
L. S. Kaplan,¹⁷³ A. Kapliy,³¹ D. Kar,⁵³ K. Karakostas,¹⁰ A. Karamaoun,³ N. Karastathis,^{10,107} M. J. Kareem,⁵⁴ E. Karentzos,¹⁰
M. Karnevskiy,⁸³ S. N. Karpov,⁶⁵ Z. M. Karpova,⁶⁵ K. Karthik,¹¹⁰ V. Kartvelishvili,⁷² A. N. Karyukhin,¹³⁰ L. Kashif,¹⁷³

- R. D. Kass,¹¹¹ A. Kastanas,¹⁴ Y. Kataoka,¹⁵⁵ C. Kato,¹⁵⁵ A. Katre,⁴⁹ J. Katzy,⁴² K. Kawagoe,⁷⁰ T. Kawamoto,¹⁵⁵ G. Kawamura,⁵⁴ S. Kazama,¹⁵⁵ V. F. Kazanin,^{109,c} R. Keeler,¹⁶⁹ R. Kehoe,⁴⁰ J. S. Keller,⁴² J. J. Kempster,⁷⁷ H. Keoshkerian,⁸⁴ O. Kepka,¹²⁷ B. P. Kerševan,⁷⁵ S. Kersten,¹⁷⁵ R. A. Keyes,⁸⁷ F. Khalil-zada,¹¹ H. Khandanyan,^{146a,146b} A. Khanov,¹¹⁴ A. G. Kharlamov,^{109,c} T. J. Khoo,²⁸ V. Khovanskiy,⁹⁷ E. Khramov,⁶⁵ J. Khubua,^{51b,t} H. Y. Kim,⁸ H. Kim,^{146a,146b} S. H. Kim,¹⁶⁰ Y. Kim,³¹ N. Kimura,¹⁵⁴ O. M. Kind,¹⁶ B. T. King,⁷⁴ M. King,¹⁶⁷ S. B. King,¹⁶⁸ J. Kirk,¹³¹ A. E. Kiryunin,¹⁰¹ T. Kishimoto,⁶⁷ D. Kisielewska,^{38a} F. Kiss,⁴⁸ K. Kiuchi,¹⁶⁰ O. Kivernyk,¹³⁶ E. Kladiva,^{144b} M. H. Klein,³⁵ M. Klein,⁷⁴ U. Klein,⁷⁴ K. Kleinknecht,⁸³ P. Klimek,^{146a,146b} A. Klimentov,²⁵ R. Klingenberg,⁴³ J. A. Klinger,¹³⁹ T. Klioutchnikova,³⁰ E.-E. Kluge,^{58a} P. Kluit,¹⁰⁷ S. Kluth,¹⁰¹ J. Knapik,³⁹ E. Kneringer,⁶² E. B. F. G. Knoops,⁸⁵ A. Knue,⁵³ A. Kobayashi,¹⁵⁵ D. Kobayashi,¹⁵⁷ T. Kobayashi,¹⁵⁵ M. Kobel,⁴⁴ M. Kocian,¹⁴³ P. Kodys,²⁹ T. Koffman,¹⁰⁷ E. Koffeman,¹⁰⁷ L. A. Kogan,¹²⁰ S. Kohlmann,¹⁷⁵ Z. Kohout,¹²⁸ T. Kohriki,⁶⁶ T. Koi,¹⁴³ H. Kolanoski,¹⁶ I. Koletsou,⁵ A. A. Komar,^{96,*} Y. Komori,¹⁵⁵ T. Kondo,⁶⁶ N. Kondrashova,⁴² K. Köneke,⁴⁸ A. C. König,¹⁰⁶ T. Kono,⁶⁶ R. Konoplich,^{110,u} N. Konstantinidis,⁷⁸ R. Kopeliansky,¹⁵² S. Koperny,^{38a} L. Köpke,⁸³ A. K. Kopp,⁴⁸ K. Korcyl,³⁹ K. Kordas,¹⁵⁴ A. Korn,⁷⁸ A. A. Korol,^{109,c} I. Korolkov,¹² E. V. Korolkova,¹³⁹ O. Kortner,¹⁰¹ S. Kortner,¹⁰¹ T. Kosek,¹²⁹ V. V. Kostyukhin,²¹ V. M. Kotov,⁶⁵ A. Kotwal,⁴⁵ A. Kourkoumeli-Charalampidi,¹⁵⁴ C. Kourkoumelis,⁹ V. Kouskoura,²⁵ A. Koutsman,^{159a} R. Kowalewski,¹⁶⁹ T. Z. Kowalski,^{38a} W. Kozanecki,¹³⁶ A. S. Kozhin,¹³⁰ V. A. Kramarenko,⁹⁹ G. Kramberger,⁷⁵ D. Krasnopevtsev,⁹⁸ M. W. Krasny,⁸⁰ A. Krasznahorkay,³⁰ J. K. Kraus,²¹ A. Kravchenko,²⁵ S. Kreiss,¹¹⁰ M. Kretz,^{58c} J. Kretzschmar,⁷⁴ K. Kreutzfeldt,⁵² P. Krieger,¹⁵⁸ K. Krizka,³¹ K. Kroeninger,⁴³ H. Kroha,¹⁰¹ J. Kroll,¹²² J. Kroeseberg,²¹ J. Krstic,¹³ U. Kruchonak,⁶⁵ H. Krüger,²¹ N. Krumann,⁶⁴ A. Kruse,¹⁷³ M. C. Kruse,⁴⁵ M. Kruskal,²² T. Kubota,⁸⁸ H. Kucuk,⁷⁸ S. Kuday,^{4b} S. Kuehn,⁴⁸ A. Kugel,^{58c} F. Kuger,¹⁷⁴ A. Kuhl,¹³⁷ T. Kuhl,⁴² V. Kukhtin,⁶⁵ Y. Kulchitsky,⁹² S. Kuleshov,^{32b} M. Kuna,^{132a,132b} T. Kunigo,⁶⁸ A. Kupco,¹²⁷ H. Kurashige,⁶⁷ Y. A. Kurochkin,⁹² V. Kus,¹²⁷ E. S. Kuwertz,¹⁶⁹ M. Kuze,¹⁵⁷ J. Kvita,¹¹⁵ T. Kwan,¹⁶⁹ D. Kyriazopoulos,¹³⁹ A. La Rosa,¹³⁷ J. L. La Rosa Navarro,^{24d} L. La Rotonda,^{37a,37b} C. Lacasta,¹⁶⁷ F. Lacava,^{132a,132b} J. Lacey,²⁹ H. Lacker,¹⁶ D. Lacour,⁸⁰ V. R. Lacuesta,¹⁶⁷ E. Ladygin,⁶⁵ R. Lafaye,⁵ B. Laforge,⁸⁰ T. Lagouri,¹⁷⁶ S. Lai,⁵⁴ L. Lambourne,⁷⁸ S. Lammers,⁶¹ C. L. Lampen,⁷ W. Lampl,⁷ E. Lançon,¹³⁶ U. Landgraf,⁴⁸ M. P. J. Landon,⁷⁶ V. S. Lang,^{58a} J. C. Lange,¹² A. J. Lankford,¹⁶³ F. Lanni,²⁵ K. Lantzsch,³⁰ A. Lanza,^{121a} S. Laplace,⁸⁰ C. Lapoire,³⁰ J. F. Laporte,¹³⁶ T. Lari,^{91a} F. Lasagni Manghi,^{20a,20b} M. Lassnig,³⁰ P. Laurelli,⁴⁷ W. Lavrijzen,¹⁵ A. T. Law,¹³⁷ P. Laycock,⁷⁴ T. Lazovich,⁵⁷ O. Le Dortz,⁸⁰ E. Le Guiriec,⁸⁵ E. Le Menedeu,¹² M. LeBlanc,¹⁶⁹ T. LeCompte,⁶ F. Ledroit-Guillon,⁵⁵ C. A. Lee,^{145b} S. C. Lee,¹⁵¹ L. Lee,¹ G. Lefebvre,⁸⁰ M. Lefebvre,¹⁶⁹ F. Legger,¹⁰⁰ C. Leggett,¹⁵ A. Lehan,⁷⁴ G. Lehmann Miotto,³⁰ X. Lei,⁷ W. A. Leight,²⁹ A. Leisos,^{154,v} A. G. Leister,¹⁷⁶ M. A. L. Leite,^{24d} R. Leitner,¹²⁹ D. Lellouch,¹⁷² B. Lemmer,⁵⁴ K. J. C. Leney,⁷⁸ T. Lenz,²¹ B. Lenzi,³⁰ R. Leone,⁷ S. Leone,^{124a,124b} C. Leonidopoulos,⁴⁶ S. Leontsinis,¹⁰ C. Leroy,⁹⁵ C. G. Lester,²⁸ M. Levchenko,¹²³ J. Levêque,⁵ D. Levin,⁸⁹ L. J. Levinson,¹⁷² M. Levy,¹⁸ A. Lewis,¹²⁰ A. M. Leyko,²¹ M. Leyton,⁴¹ B. Li,^{33b,w} H. Li,¹⁴⁸ H. L. Li,³¹ L. Li,⁴⁵ L. Li,^{33e} S. Li,⁴⁵ Y. Li,^{33c,x} Z. Liang,¹³⁷ H. Liao,³⁴ B. Liberti,^{133a} A. Liblong,¹⁵⁸ P. Lichard,³⁰ K. Lie,¹⁶⁵ J. Liebal,²¹ W. Liebig,¹⁴ C. Limbach,²¹ A. Limosani,¹⁵⁰ S. C. Lin,^{151,y} T. H. Lin,⁸³ F. Linde,¹⁰⁷ B. E. Lindquist,¹⁴⁸ J. T. Linnemann,⁹⁰ E. Lipeles,¹²² A. Lipniacka,¹⁴ M. Lisoviy,^{58b} T. M. Liss,¹⁶⁵ D. Lissauer,²⁵ A. Lister,¹⁶⁸ A. M. Litke,¹³⁷ B. Liu,^{151,z} D. Liu,¹⁵¹ H. Liu,⁸⁹ J. Liu,⁸⁵ J. B. Liu,^{33b} K. Liu,⁸⁵ L. Liu,¹⁶⁵ M. Liu,⁴⁵ M. Liu,^{33b} Y. Liu,^{33b} M. Livan,^{121a,121b} A. Lleres,⁵⁵ J. Llorente Merino,⁸² S. L. Lloyd,⁷⁶ F. Lo Sterzo,¹⁵¹ E. Lobodzinska,⁴² P. Loch,⁷ W. S. Lockman,¹³⁷ F. K. Loebinger,⁸⁴ A. E. Loevschall-Jensen,³⁶ A. Loginov,¹⁷⁶ T. Lohse,¹⁶ K. Lohwasser,⁴² M. Lokajicek,¹²⁷ B. A. Long,²² J. D. Long,⁸⁹ R. E. Long,⁷² K. A. Looper,¹¹¹ L. Lopes,^{126a} D. Lopez Mateos,⁵⁷ B. Lopez Paredes,¹³⁹ I. Lopez Paz,¹² J. Lorenz,¹⁰⁰ N. Lorenzo Martinez,⁶¹ M. Losada,¹⁶² P. Loscutoff,¹⁵ P. J. Lösel,¹⁰⁰ X. Lou,^{33a} A. Lounis,¹¹⁷ J. Love,⁶ P. A. Love,⁷² N. Lu,⁸⁹ H. J. Lubatti,¹³⁸ C. Luci,^{132a,132b} A. Lucotte,⁵⁵ F. Luehring,⁶¹ W. Lukas,⁶² L. Luminari,^{132a} O. Lundberg,^{146a,146b} B. Lund-Jensen,¹⁴⁷ D. Lynn,²⁵ R. Lysak,¹²⁷ E. Lytken,⁸¹ H. Ma,²⁵ L. L. Ma,^{33d} G. Maccarrone,⁴⁷ A. Macchiolo,¹⁰¹ C. M. Macdonald,¹³⁹ J. Machado Miguens,^{122,126b} D. Macina,³⁰ D. Madaffari,⁸⁵ R. Madar,³⁴ H. J. Maddocks,⁷² W. F. Mader,⁴⁴ A. Madsen,¹⁶⁶ S. Maeland,¹⁴ T. Maeno,²⁵ A. Maevskiy,⁹⁹ E. Magradze,⁵⁴ K. Mahboubi,⁴⁸ J. Mahlstedt,¹⁰⁷ C. Maiani,¹³⁶ C. Maidantchik,^{24a} A. A. Maier,¹⁰¹ T. Maier,¹⁰⁰ A. Maio,^{126a,126b,126d} S. Majewski,¹¹⁶ Y. Makida,⁶⁶ N. Makovec,¹¹⁷ B. Malaescu,⁸⁰ Pa. Malecki,³⁹ V. P. Maleev,¹²³ F. Malek,⁵⁵ U. Mallik,⁶³ D. Malon,⁶ C. Malone,¹⁴³ S. Maltezos,¹⁰ V. M. Malyshev,¹⁰⁹ S. Malyukov,³⁰ J. Mamuzic,⁴² G. Mancini,⁴⁷ B. Mandelli,³⁰ L. Mandelli,^{91a} I. Mandić,⁷⁵ R. Mandrysch,⁶³ J. Maneira,^{126a,126b} A. Manfredini,¹⁰¹ L. Manhaes de Andrade Filho,^{24b} J. Manjarres Ramos,^{159b} A. Mann,¹⁰⁰ P. M. Manning,¹³⁷ A. Manousakis-Katsikakis,⁹ B. Mansoulie,¹³⁶ R. Mantifel,⁸⁷ M. Mantoani,⁵⁴ L. Mapelli,³⁰ L. March,^{145c} G. Marchiori,⁸⁰ M. Marcisovsky,¹²⁷ C. P. Marino,¹⁶⁹ M. Marjanovic,¹³ D. E. Marley,⁸⁹ F. Marroquim,^{24a} S. P. Marsden,⁸⁴ Z. Marshall,¹⁵ L. F. Marti,¹⁷ S. Marti-Garcia,¹⁶⁷ B. Martin,⁹⁰ T. A. Martin,¹⁷⁰ V. J. Martin,⁴⁶ B. Martin dit Latour,¹⁴ M. Martinez,^{12,o} S. Martin-Haugh,¹³¹ V. S. Martoiu,^{26a} A. C. Martyniuk,⁷⁸ M. Marx,¹³⁸ F. Marzano,^{132a} A. Marzin,³⁰ L. Masetti,⁸³ T. Mashimo,¹⁵⁵ R. Mashinistov,⁹⁶ J. Masik,⁸⁴ A. L. Maslenikov,^{109,c} I. Massa,^{20a,20b} L. Massa,^{20a,20b} N. Massol,⁵ P. Mastrandrea,¹⁴⁸ A. Mastroberardino,^{37a,37b} T. Masubuchi,¹⁵⁵ P. Mättig,¹⁷⁵ J. Mattmann,⁸³ J. Maurer,^{26a} S. J. Maxfield,⁷⁴ D. A. Maximov,^{109,c} R. Mazini,¹⁵¹ S. M. Mazza,^{91a,91b} L. Mazzaferro,^{133a,133b} G. Mc Goldrick,¹⁵⁸ S. P. Mc Kee,⁸⁹ A. McCarn,⁸⁹ R. L. McCarthy,¹⁴⁸ T. G. McCarthy,²⁹ N. A. McCubbin,¹³¹ K. W. McFarlane,^{56,*} J. A. McFayden,⁷⁸ G. Mchedlidze,⁵⁴ S. J. McMahon,¹³¹ R. A. McPherson,^{169,k} M. Medinnis,⁴² S. Meehan,^{145a} S. Mehlhase,¹⁰⁰ A. Mehta,⁷⁴ K. Meier,^{58a} C. Meineck,¹⁰⁰ B. Meirose,⁴¹ B. R. Mellado Garcia,^{145c} F. Meloni,¹⁷ A. Mengarelli,^{20a,20b} S. Menke,¹⁰¹ E. Meoni,¹⁶¹ K. M. Mercurio,⁵⁷ S. Mergelmeyer,²¹ P. Mermod,⁴⁹ L. Merola,^{104a,104b} C. Meroni,^{91a} F. S. Merritt,³¹ A. Messina,^{132a,132b} J. Metcalfe,²⁵ A. S. Mete,¹⁶³ C. Meyer,⁸³ C. Meyer,¹²² J-P. Meyer,¹³⁶ J. Meyer,¹⁰⁷ R. P. Middleton,¹³¹ S. Miglioranzi,^{164a,164c} L. Mijović,²¹ G. Mikenberg,¹⁷² M. Mikestikova,¹²⁷ M. Mikuž,⁷⁵ M. Milesi,⁸⁸ A. Milic,³⁰ D. W. Miller,³¹

- C. Mills,⁴⁶ A. Milov,¹⁷² D. A. Milstead,^{146a,146b} A. A. Minaenko,¹³⁰ Y. Minami,¹⁵⁵ I. A. Minashvili,⁶⁵ A. I. Mincer,¹¹⁰
 B. Mindur,^{38a} M. Mineev,⁶⁵ Y. Ming,¹⁷³ L. M. Mir,¹² T. Mitani,¹⁷¹ J. Mitrevski,¹⁰⁰ V. A. Mitsou,¹⁶⁷ A. Miucci,⁴⁹
 P. S. Miyagawa,¹³⁹ J. U. Mjörnmark,⁸¹ T. Moa,^{146a,146b} K. Mochizuki,⁸⁵ S. Mohapatra,³⁵ W. Mohr,⁴⁸ S. Molander,^{146a,146b}
 R. Moles-Valls,²¹ K. Möning,⁴² C. Monini,⁵⁵ J. Monk,³⁶ E. Monnier,⁸⁵ J. Montejo Berlingen,¹² F. Monticelli,⁷¹
 S. Monzani,^{132a,132b} R. W. Moore,³ N. Morange,¹¹⁷ D. Moreno,¹⁶² M. Moreno Llácer,⁵⁴ P. Morettini,^{50a} M. Morgenstern,⁴⁴
 D. Mori,¹⁴² M. Morii,⁵⁷ M. Morinaga,¹⁵⁵ V. Morisbak,¹¹⁹ S. Moritz,⁸³ A. K. Morley,¹⁵⁰ G. Mornacchi,³⁰ J. D. Morris,⁷⁶
 S. S. Mortensen,³⁶ A. Morton,⁵³ L. Morvaj,¹⁰³ M. Mosidze,^{51b} J. Moss,¹¹¹ K. Motohashi,¹⁵⁷ R. Mount,¹⁴³ E. Mountricha,²⁵
 S. V. Mouraviev,^{96,*} E. J. W. Moyse,⁸⁶ S. Muanza,⁸⁵ R. D. Mudd,¹⁸ F. Mueller,¹⁰¹ J. Mueller,¹²⁵ R. S. P. Mueller,¹⁰⁰
 T. Mueller,²⁸ D. Muenstermann,⁴⁹ P. Mullen,⁵³ G. A. Mullier,¹⁷ J. A. Murillo Quijada,¹⁸ W. J. Murray,^{170,131} H. Musheghyan,⁵⁴
 E. Musto,¹⁵² A. G. Myagkov,^{130,aa} M. Myska,¹²⁸ B. P. Nachman,¹⁴³ O. Nackenhorst,⁵⁴ J. Nadal,⁵⁴ K. Nagai,¹²⁰ R. Nagai,¹⁵⁷
 Y. Nagai,⁸⁵ K. Nagano,⁶⁶ A. Nagarkar,¹¹¹ Y. Nagasaka,⁵⁹ K. Nagata,¹⁶⁰ M. Nagel,¹⁰¹ E. Nagy,⁸⁵ A. M. Nairz,³⁰ Y. Nakahama,³⁰
 K. Nakamura,⁶⁶ T. Nakamura,¹⁵⁵ I. Nakano,¹¹² H. Namasivayam,⁴¹ R. F. Naranjo Garcia,⁴² R. Narayan,³¹ T. Naumann,⁴²
 G. Navarro,¹⁶² R. Nayyar,⁷ H. A. Neal,⁸⁹ P. Yu. Nechaeva,⁹⁶ T. J. Neep,⁸⁴ P. D. Nef,¹⁴³ A. Negri,^{121a,121b} M. Negrini,^{20a}
 S. Nektarijevic,¹⁰⁶ C. Nellist,¹¹⁷ A. Nelson,¹⁶³ S. Nemecek,¹²⁷ P. Nemethy,¹¹⁰ A. A. Nepomuceno,^{24a} M. Nessi,^{30,ab}
 M. S. Neubauer,¹⁶⁵ M. Neumann,¹⁷⁵ R. M. Neves,¹¹⁰ P. Nevski,²⁵ P. R. Newman,¹⁸ D. H. Nguyen,⁶ R. B. Nickerson,¹²⁰
 R. Nicolaïdou,¹³⁶ B. Nicquevert,³⁰ J. Nielsen,¹³⁷ N. Nikiforou,³⁵ A. Nikiforov,¹⁶ V. Nikolaenko,^{130,aa} I. Nikolic-Audit,⁸⁰
 K. Nikolopoulos,¹⁸ J. K. Nilsen,¹¹⁹ P. Nilsson,²⁵ Y. Ninomiya,¹⁵⁵ A. Nisati,^{132a} R. Nisius,¹⁰¹ T. Nobe,¹⁵⁵ M. Nomachi,¹¹⁸
 I. Nomidis,²⁹ T. Nooney,⁷⁶ S. Norberg,¹¹³ M. Nordberg,³⁰ O. Novgorodova,⁴⁴ S. Nowak,¹⁰¹ M. Nozaki,⁶⁶ L. Nozka,¹¹⁵
 K. Ntekas,¹⁰ G. Nunes Hanninger,⁸⁸ T. Nunnemann,¹⁰⁰ E. Nurse,⁷⁸ F. Nuti,⁸⁸ B. J. O'Brien,⁴⁶ F. O'grady,⁷ D. C. O'Neil,¹⁴²
 V. O'Shea,⁵³ F. G. Oakham,^{29,d} H. Oberlack,¹⁰¹ T. Obermann,²¹ J. Ocariz,⁸⁰ A. Ochi,⁶⁷ I. Ochoa,⁷⁸ J. P. Ochoa-Ricoux,^{32a}
 S. Oda,⁷⁰ S. Odaka,⁶⁶ H. Ogren,⁶¹ A. Oh,⁸⁴ S. H. Oh,⁴⁵ C. C. Ohm,¹⁵ H. Ohman,¹⁶⁶ H. Oide,³⁰ W. Okamura,¹¹⁸ H. Okawa,¹⁶⁰
 Y. Okumura,³¹ T. Okuyama,⁶⁶ A. Olariu,^{26a} S. A. Olivares Pino,⁴⁶ D. Oliveira Damazio,²⁵ E. Oliver Garcia,¹⁶⁷ A. Olszewski,³⁹
 J. Olszowska,³⁹ A. Onofre,^{126a,126e} P. U. E. Onyisi,^{31,q} C. J. Oram,^{159a} M. J. Oreglia,³¹ Y. Oren,¹⁵³ D. Orestano,^{134a,134b}
 N. Orlando,¹⁵⁴ C. Oropeza Barrera,⁵³ R. S. Orr,¹⁵⁸ B. Osculati,^{50a,50b} R. Ospanov,⁸⁴ G. Otero y Garzon,²⁷ H. Otono,⁷⁰
 M. Ouchrif,^{135d} E. A. Ouellette,¹⁶⁹ F. Ould-Saada,¹¹⁹ A. Ouraou,¹³⁶ K. P. Oussoren,¹⁰⁷ Q. Ouyang,^{33a} A. Ovcharova,¹⁵
 M. Owen,⁵³ R. E. Owen,¹⁸ V. E. Ozcan,^{19a} N. Ozturk,⁸ K. Pachal,¹⁴² A. Pacheco Pages,¹² C. Padilla Aranda,¹² M. Pagáčová,⁴⁸
 S. Pagan Griso,¹⁵ E. Paganis,¹³⁹ F. Paige,²⁵ P. Pais,⁸⁶ K. Pajchel,¹¹⁹ G. Palacino,^{159b} S. Palestini,³⁰ M. Palka,^{38b} D. Pallin,³⁴
 A. Palma,^{126a,126b} Y. B. Pan,¹⁷³ E. Panagiotopoulou,¹⁰ C. E. Pandini,⁸⁰ J. G. Panduro Vazquez,⁷⁷ P. Pani,^{146a,146b} S. Panitkin,²⁵
 D. Pantea,^{26a} L. Paolozzi,⁴⁹ Th. D. Papadopoulou,¹⁰ K. Papageorgiou,¹⁵⁴ A. Paramonov,⁶ D. Paredes Hernandez,¹⁵⁴
 M. A. Parker,²⁸ K. A. Parker,¹³⁹ F. Parodi,^{50a,50b} J. A. Parsons,³⁵ U. Parzefall,⁴⁸ E. Pasqualucci,^{132a} S. Passaggio,^{50a}
 F. Pastore,^{134a,134b,*} Fr. Pastore,⁷⁷ G. Pásztor,²⁹ S. Pataraia,¹⁷⁵ N. D. Patel,¹⁵⁰ J. R. Pater,⁸⁴ T. Pauly,³⁰ J. Pearce,¹⁶⁹
 B. Pearson,¹¹³ L. E. Pedersen,³⁶ M. Pedersen,¹¹⁹ S. Pedraza Lopez,¹⁶⁷ R. Pedro,^{126a,126b} S. V. Peleganchuk,^{109,c} D. Pelikan,¹⁶⁶
 O. Penc,¹²⁷ C. Peng,^{33a} H. Peng,^{33b} B. Penning,³¹ J. Penwell,⁶¹ D. V. Perepelitsa,²⁵ E. Perez Codina,^{159a}
 M. T. Pérez García-Estañ,¹⁶⁷ L. Perini,^{91a,91b} H. Pernegger,³⁰ S. Perrella,^{104a,104b} R. Peschke,⁴² V. D. Peshekhanov,⁶⁵
 K. Peters,³⁰ R. F. Y. Peters,⁸⁴ B. A. Petersen,³⁰ T. C. Petersen,³⁶ E. Petit,⁴² A. Petridis,^{146a,146b} C. Petridou,¹⁵⁴ P. Petroff,¹¹⁷
 E. Petrolo,^{132a} F. Petrucci,^{134a,134b} N. E. Pettersson,¹⁵⁷ R. Pezoa,^{32b} P. W. Phillips,¹³¹ G. Piacquadio,¹⁴³ E. Pianori,¹⁷⁰
 A. Picazio,⁴⁹ E. Piccaro,⁷⁶ M. Piccinini,^{20a,20b} M. A. Pickering,¹²⁰ R. Piegaia,²⁷ D. T. Pignotti,¹¹¹ J. E. Pilcher,³¹
 A. D. Pilkington,⁸⁴ J. Pina,^{126a,126b,126d} M. Pinamonti,^{164a,164c,ac} J. L. Pinfold,³ A. Pingel,³⁶ B. Pinto,^{126a} S. Pires,⁸⁰
 H. Pirumov,⁴² M. Pitt,¹⁷² C. Pizio,^{91a,91b} L. Plazak,^{144a} M.-A. Pleier,²⁵ V. Pleskot,¹²⁹ E. Plotnikova,⁶⁵ P. Pluciński,^{146a,146b}
 D. Pluth,⁶⁴ R. Poettgen,^{146a,146b} L. Poggiali,¹¹⁷ D. Pohl,²¹ G. Polesello,^{121a} A. Poley,⁴² A. Policicchio,^{37a,37b} R. Polifka,¹⁵⁸
 A. Polini,^{20a} C. S. Pollard,⁵³ V. Polychronakos,²⁵ K. Pommès,³⁰ L. Pontecorvo,^{132a} B. G. Pope,⁹⁰ G. A. Popeneciu,^{26b}
 D. S. Popovic,¹³ A. Poppleton,³⁰ S. Pospisil,¹²⁸ K. Potamianos,¹⁵ I. N. Potrap,⁶⁵ C. J. Potter,¹⁴⁹ C. T. Potter,¹¹⁶ G. Poulard,³⁰
 J. Poveda,³⁰ V. Pozdnyakov,⁶⁵ P. Pralavorio,⁸⁵ A. Pranko,¹⁵ S. Prasad,³⁰ S. Prell,⁶⁴ D. Price,⁸⁴ L. E. Price,⁶ M. Primavera,^{73a}
 S. Prince,⁸⁷ M. Proissl,⁴⁶ K. Prokofiev,^{60c} F. Prokoshin,^{32b} E. Protopapadaki,¹³⁶ S. Protopopescu,²⁵ J. Proudfoot,⁶
 M. Przybycien,^{38a} E. Ptacek,¹¹⁶ D. Puddu,^{134a,134b} E. Pueschel,⁸⁶ D. Puldon,¹⁴⁸ M. Purohit,^{25,ad} P. Puzo,¹¹⁷ J. Qian,⁸⁹ G. Qin,⁵³
 Y. Qin,⁸⁴ A. Quadt,⁵⁴ D. R. Quarrie,¹⁵ W. B. Quayle,^{164a,164b} M. Queitsch-Maitland,⁸⁴ D. Quilty,⁵³ S. Raddum,¹¹⁹ V. Radeka,²⁵
 V. Radescu,⁴² S. K. Radhakrishnan,¹⁴⁸ P. Radloff,¹¹⁶ P. Rados,⁸⁸ F. Ragusa,^{91a,91b} G. Rahal,¹⁷⁸ S. Rajagopalan,²⁵
 M. Rammensee,³⁰ C. Rangel-Smith,¹⁶⁶ F. Rauscher,¹⁰⁰ S. Rave,⁸³ T. Ravenscroft,⁵³ M. Raymond,³⁰ A. L. Read,¹¹⁹
 N. P. Readioff,⁷⁴ D. M. Rebuzzi,^{121a,121b} A. Redelbach,¹⁷⁴ G. Redlinger,²⁵ R. Reece,¹³⁷ K. Reeves,⁴¹ L. Rehnisch,¹⁶
 J. Reichert,¹²² H. Reisin,²⁷ M. Relich,¹⁶³ C. Rembser,³⁰ H. Ren,^{33a} A. Renaud,¹¹⁷ M. Rescigno,^{132a} S. Resconi,^{91a}
 O. L. Rezanova,^{109,c} P. Reznicek,¹²⁹ R. Rezvani,⁹⁵ R. Richter,¹⁰¹ S. Richter,⁷⁸ E. Richter-Was,^{38b} O. Ricken,²¹ M. Ridel,⁸⁰
 P. Rieck,¹⁶ C. J. Riegel,¹⁷⁵ J. Rieger,⁵⁴ M. Rijssenbeek,¹⁴⁸ A. Rimoldi,^{121a,121b} L. Rinaldi,^{20a} B. Ristić,⁴⁹ E. Ritsch,³⁰ I. Riu,¹²
 F. Rizatdinova,¹¹⁴ E. Rizvi,⁷⁶ S. H. Robertson,^{87,k} A. Robichaud-Veronneau,⁸⁷ D. Robinson,²⁸ J. E. M. Robinson,⁴²
 A. Robson,⁵³ C. Roda,^{124a,124b} S. Roe,³⁰ O. Røhne,¹¹⁹ S. Rolli,¹⁶¹ A. Romaniouk,⁹⁸ M. Romano,^{20a,20b} S. M. Romano Saez,³⁴
 E. Romero Adam,¹⁶⁷ N. Rompotis,¹³⁸ M. Ronzani,⁴⁸ L. Roos,⁸⁰ E. Ros,¹⁶⁷ S. Rosati,^{132a} K. Rosbach,⁴⁸ P. Rose,¹³⁷
 P. L. Rosendahl,¹⁴ O. Rosenthal,¹⁴¹ V. Rossetti,^{146a,146b} E. Rossi,^{104a,104b} L. P. Rossi,^{50a} R. Rosten,¹³⁸ M. Rotaru,^{26a} I. Roth,¹⁷²
 J. Rothberg,¹³⁸ D. Rousseau,¹¹⁷ C. R. Royon,¹³⁶ A. Rozanov,⁸⁵ Y. Rozen,¹⁵² X. Ruan,^{145c} F. Rubbo,¹⁴³ I. Rubinskiy,⁴²
 V. I. Rud,⁹⁹ C. Rudolph,⁴⁴ M. S. Rudolph,¹⁵⁸ F. Rühr,⁴⁸ A. Ruiz-Martinez,³⁰ Z. Rurikova,⁴⁸ N. A. Rusakovich,⁶⁵ A. Ruschke,¹⁰⁰

- H. L. Russell,¹³⁸ J. P. Rutherford,⁷ N. Ruthmann,⁴⁸ Y. F. Ryabov,¹²³ M. Rybar,¹⁶⁵ G. Rybkin,¹¹⁷ N. C. Ryder,¹²⁰
A. F. Saavedra,¹⁵⁰ G. Sabato,¹⁰⁷ S. Sacerdoti,²⁷ A. Saddique,³ H. F.-W. Sadrozinski,¹³⁷ R. Sadykov,⁶⁵ F. Safai Tehrani,^{132a}
M. Sahinsoy,^{19a} M. Saimpert,¹³⁶ T. Saito,¹⁵⁵ H. Sakamoto,¹⁵⁵ Y. Sakurai,¹⁷¹ G. Salamanna,^{134a,134b} A. Salamon,^{133a}
M. Saleem,¹¹³ D. Salek,¹⁰⁷ P. H. Sales De Bruin,¹³⁸ D. Salihagic,¹⁰¹ A. Salnikov,¹⁴³ J. Salt,¹⁶⁷ D. Salvatore,^{37a,37b}
F. Salvatore,¹⁴⁹ A. Salvucci,¹⁰⁶ A. Salzburger,³⁰ D. Sammel,⁴⁸ D. Sampsonidis,¹⁵⁴ A. Sanchez,^{104a,104b} J. Sanchez,¹⁶⁷
V. Sanchez Martinez,¹⁶⁷ H. Sandaker,¹¹⁹ R. L. Sandbach,⁷⁶ H. G. Sander,⁸³ M. P. Sanders,¹⁰⁰ M. Sandhoff,¹⁷⁵ C. Sandoval,¹⁶²
R. Sandstroem,¹⁰¹ D. P. C. Sankey,¹³¹ M. Sannino,^{50a,50b} A. Sansoni,⁴⁷ C. Santoni,³⁴ R. Santonico,^{133a,133b} H. Santos,^{126a}
I. Santoyo Castillo,¹⁴⁹ K. Sapp,¹²⁵ A. Sapronov,⁶⁵ J. G. Saraiva,^{126a,126d} B. Sarrazin,²¹ O. Sasaki,⁶⁶ Y. Sasaki,¹⁵⁵ K. Sato,¹⁶⁰
G. Sauvage,^{5,*} E. Sauvan,⁵ G. Savage,⁷⁷ P. Savard,^{158,d} C. Sawyer,¹³¹ L. Sawyer,^{79,n} J. Saxon,³¹ C. Sbarra,^{20a} A. Sbrizzi,^{20a,20b}
T. Scanlon,⁷⁸ D. A. Scannicchio,¹⁶³ M. Scarcella,¹⁵⁰ V. Scarfone,^{37a,37b} J. Schaarschmidt,¹⁷² P. Schacht,¹⁰¹ D. Schaefer,³⁰
R. Schaefer,⁴² J. Schaeffer,⁸³ S. Schaepe,²¹ S. Schaetzle,^{58b} U. Schäfer,⁸³ A. C. Schaffer,¹¹⁷ D. Schaire,¹⁰⁰
R. D. Schamberger,¹⁴⁸ V. Scharf,^{58a} V. A. Schegelsky,¹²³ D. Scheirich,¹²⁹ M. Schernau,¹⁶³ C. Schiavi,^{50a,50b} C. Schillo,⁴⁸
M. Schioppa,^{37a,37b} S. Schlenker,³⁰ E. Schmidt,⁴⁸ K. Schmieden,³⁰ C. Schmitt,⁸³ S. Schmitt,^{58b} S. Schmitt,⁴² B. Schneider,^{159a}
Y. J. Schnellbach,⁷⁴ U. Schnoor,⁴⁴ L. Schoeffel,¹³⁶ A. Schoening,^{58b} B. D. Schoenrock,⁹⁰ E. Schopf,²¹ A. L. S. Schorlemmer,⁵⁴
M. Schott,⁸³ D. Schouten,^{159a} J. Schovancova,⁸ S. Schramm,⁴⁹ M. Schreyer,¹⁷⁴ C. Schroeder,⁸³ N. Schuh,⁸³ M. J. Schultens,²¹
H.-C. Schultz-Coulon,^{58a} H. Schulz,¹⁶ M. Schumacher,⁴⁸ B. A. Schumm,¹³⁷ Ph. Schune,¹³⁶ C. Schwanenberger,⁸⁴
A. Schwartzman,¹⁴³ T. A. Schwarz,⁸⁹ Ph. Schwegler,¹⁰¹ H. Schweiger,⁸⁴ Ph. Schwemling,¹³⁶ R. Schwienhorst,⁹⁰
J. Schwindling,¹³⁶ T. Schwindt,²¹ F. G. Sciaccia,¹⁷ E. Scifo,¹¹⁷ G. Sciolla,²³ F. Scuri,^{124a,124b} F. Scutti,²¹ J. Searcy,⁸⁹ G. Sedov,⁴²
E. Sedykh,¹²³ P. Seema,²¹ S. C. Seidel,¹⁰⁵ A. Seiden,¹³⁷ F. Seifert,¹²⁸ J. M. Seixas,^{24a} G. Sekhniaidze,^{104a} K. Sekhon,⁸⁹
S. J. Sekula,⁴⁰ D. M. Seliverstov,^{123,*} N. Semprini-Cesari,^{20a,20b} C. Serfon,³⁰ L. Serin,¹¹⁷ L. Serkin,^{164a,164b} T. Serre,⁸⁵
M. Sessa,^{134a,134b} R. Seuster,^{159a} H. Severini,¹¹³ T. Sfiligoj,⁷⁵ F. Sforza,³⁰ A. Sfyrla,³⁰ E. Shabalina,⁵⁴ M. Shamim,¹¹⁶
L. Y. Shan,^{33a} R. Shang,¹⁶⁵ J. T. Shank,²² M. Shapiro,¹⁵ P. B. Shatalov,⁹⁷ K. Shaw,^{164a,164b} S. M. Shaw,⁸⁴
A. Shcherbakova,^{146a,146b} C. Y. Shehu,¹⁴⁹ P. Sherwood,⁷⁸ L. Shi,^{151,ae} S. Shimizu,⁶⁷ C. O. Shimmin,¹⁶³ M. Shimojima,¹⁰²
M. Shiyakova,⁶⁵ A. Shmeleva,⁹⁶ D. Shoaleh Saadi,⁹⁵ M. J. Shochet,³¹ S. Shoajii,^{91a,91b} S. Shrestha,¹¹¹ E. Shulga,⁹⁸
M. A. Shupe,⁷ S. Shushkevich,⁴² P. Sicho,¹²⁷ P. E. Sidebo,¹⁴⁷ O. Sidiropoulou,¹⁷⁴ D. Sidorov,¹¹⁴ A. Sidoti,^{20a,20b} F. Siegert,⁴⁴
Dj. Sijacki,¹³ J. Silva,^{126a,126d} Y. Silver,¹⁵³ S. B. Silverstein,^{146a} V. Simak,¹²⁸ O. Simard,⁵ Lj. Simic,¹³ S. Simion,¹¹⁷
E. Simioni,⁸³ B. Simmons,⁷⁸ D. Simon,³⁴ R. Simoniello,^{91a,91b} P. Sinervo,¹⁵⁸ N. B. Sinev,¹¹⁶ M. Sioli,^{20a,20b} G. Siragusa,¹⁷⁴
A. N. Sisakyan,^{65,*} S. Yu. Sivoklokov,⁹⁹ J. Sjölin,^{146a,146b} T. B. Sjursen,¹⁴ M. B. Skinner,⁷² H. P. Skottowe,⁵⁷ P. Skubic,¹¹³
M. Slater,¹⁸ T. Slavicek,¹²⁸ M. Slawinska,¹⁰⁷ K. Sliwa,¹⁶¹ V. Smakhtin,¹⁷² B. H. Smart,⁴⁶ L. Smestad,¹⁴ S. Yu. Smirnov,⁹⁸
Y. Smirnov,⁹⁸ L. N. Smirnova,^{99,af} O. Smirnova,⁸¹ M. N. K. Smith,³⁵ R. W. Smith,³⁵ M. Smizanska,⁷² K. Smolek,¹²⁸
A. A. Snesarev,⁹⁶ G. Snidero,⁷⁶ S. Snyder,²⁵ R. Sobie,^{169,k} F. Socher,⁴⁴ A. Soffer,¹⁵³ D. A. Soh,^{151,ae} C. A. Solans,³⁰
M. Solar,¹²⁸ J. Solc,¹²⁸ E. Yu. Soldatov,⁹⁸ U. Soldevila,¹⁶⁷ A. A. Solodkov,¹³⁰ A. Soloshenko,⁶⁵ O. V. Solovyanov,¹³⁰
V. Solovyev,¹²³ P. Sommer,⁴⁸ H. Y. Song,^{33b} N. Soni,¹ A. Sood,¹⁵ A. Sopczak,¹²⁸ B. Sopko,¹²⁸ V. Sopko,¹²⁸ V. Sorin,¹²
D. Sosa,^{58b} M. Sosebee,⁸ C. L. Sotiropoulou,^{124a,124b} R. Soualah,^{164a,164c} A. M. Soukharev,^{109,c} D. South,⁴² B. C. Sowden,⁷⁷
S. Spagnolo,^{73a,73b} M. Spalla,^{124a,124b} F. Spanò,⁷⁷ W. R. Spearman,⁵⁷ D. Sperlich,¹⁶ F. Spettel,¹⁰¹ R. Spighi,^{20a} G. Spigo,³⁰
L. A. Spiller,⁸⁸ M. Spousta,¹²⁹ T. Spreitzer,¹⁵⁸ R. D. St. Denis,^{53,*} S. Staerz,⁴⁴ J. Stahlman,¹²² R. Stamen,^{58a} S. Stamm,¹⁶
E. Stancka,³⁹ C. Stanescu,^{134a} M. Stanescu-Bellu,⁴² M. M. Stanitzki,⁴² S. Stapnes,¹¹⁹ E. A. Starchenko,¹³⁰ J. Stark,⁵⁵
P. Staroba,¹²⁷ P. Starovoitov,⁴² R. Staszewski,³⁹ P. Stavina,^{144a,*} P. Steinberg,²⁵ B. Stelzer,¹⁴² H. J. Stelzer,³⁰
O. Stelzer-Chilton,^{159a} H. Stenzel,⁵² G. A. Stewart,⁵³ J. A. Stillings,²¹ M. C. Stockton,⁸⁷ M. Stoebe,⁸⁷ G. Stoica,^{26a} P. Stolte,⁵⁴
S. Stonjek,¹⁰¹ A. R. Stradling,⁸ A. Straessner,⁴⁴ M. E. Stramaglia,¹⁷ J. Strandberg,¹⁴⁷ S. Strandberg,^{146a,146b} A. Strandlie,¹¹⁹
E. Strauss,¹⁴³ M. Strauss,¹¹³ P. Strizenec,^{144b} R. Ströhmer,¹⁷⁴ D. M. Strom,¹¹⁶ R. Stroynowski,⁴⁰ A. Strubig,¹⁰⁶ S. A. Stucci,¹⁷
B. Stugu,¹⁴ N. A. Styles,⁴² D. Su,¹⁴³ J. Su,¹²⁵ R. Subramaniam,⁷⁹ A. Succurro,¹² Y. Sugaya,¹¹⁸ C. Suhr,¹⁰⁸ M. Suk,¹²⁸
V. V. Sulin,⁹⁶ S. Sultansoy,^{4c} T. Sumida,⁶⁸ S. Sun,⁵⁷ X. Sun,^{33a} J. E. Sundermann,⁴⁸ K. Suruliz,¹⁴⁹ G. Susinno,^{37a,37b}
M. R. Sutton,¹⁴⁹ S. Suzuki,⁶⁶ M. Svatos,¹²⁷ S. Swedish,¹⁶⁸ M. Swiatlowski,¹⁴³ I. Sykora,^{144a} T. Sykora,¹²⁹ D. Ta,⁹⁰
C. Taccini,^{134a,134b} K. Tackmann,⁴² J. Taenzer,¹⁵⁸ A. Taffard,¹⁶³ R. Tafirout,^{159a} N. Taiblum,¹⁵³ H. Takai,²⁵ R. Takashima,⁶⁹
H. Takeda,⁶⁷ T. Takeshita,¹⁴⁰ Y. Takubo,⁶⁶ M. Talby,⁸⁵ A. A. Talyshov,^{109,c} J. Y. C. Tam,¹⁷⁴ K. G. Tan,⁸⁸ J. Tanaka,¹⁵⁵
R. Tanaka,¹¹⁷ S. Tanaka,⁶⁶ B. B. Tannenwald,¹¹¹ N. Tannoury,²¹ S. Tapprogge,⁸³ S. Tarem,¹⁵² F. Tarrade,²⁹ G. F. Tartarelli,^{91a}
P. Tas,¹²⁹ M. Tasevsky,¹²⁷ T. Tashiro,⁶⁸ E. Tassi,^{37a,37b} A. Tavares Delgado,^{126a,126b} Y. Tayalati,^{135d} F. E. Taylor,⁹⁴
G. N. Taylor,⁸⁸ W. Taylor,^{159b} F. A. Teischinger,³⁰ M. Teixeira Dias Castanheira,⁷⁶ P. Teixeira-Dias,⁷⁷ K. K. Temming,⁴⁸
H. Ten Kate,³⁰ P. K. Teng,¹⁵¹ J. J. Teoh,¹¹⁸ F. Tepel,¹⁷⁵ S. Terada,⁶⁶ K. Terashi,¹⁵⁵ J. Terron,⁸² S. Terzo,¹⁰¹ M. Testa,⁴⁷
R. J. Teuscher,^{158,k} T. Theveneaux-Pelzer,³⁴ J. P. Thomas,¹⁸ J. Thomas-Wilsker,⁷⁷ E. N. Thompson,³⁵ P. D. Thompson,¹⁸
R. J. Thompson,⁸⁴ A. S. Thompson,⁵³ L. A. Thomsen,¹⁷⁶ E. Thomson,¹²² M. Thomson,²⁸ R. P. Thun,^{89,*} M. J. Tibbetts,¹⁵
R. E. Ticse Torres,⁸⁵ V. O. Tikhomirov,^{96,ag} Yu. A. Tikhonov,^{109,c} S. Timoshenko,⁹⁸ E. Tiouchichine,⁸⁵ P. Tipton,¹⁷⁶
S. Tisserant,⁸⁵ K. Todome,¹⁵⁷ T. Todorov,^{5,*} S. Todorova-Nova,¹²⁹ J. Tojo,⁷⁰ S. Tokár,^{144a} K. Tokushuku,⁶⁶ K. Tollefson,⁹⁰
E. Tolley,⁵⁷ L. Tomlinson,⁸⁴ M. Tomoto,¹⁰³ L. Tompkins,^{143,ah} K. Toms,¹⁰⁵ E. Torrence,¹¹⁶ H. Torres,¹⁴² E. Torró Pastor,¹⁶⁷
J. Toth,^{85,ai} F. Touchard,⁸⁵ D. R. Tovey,¹³⁹ T. Trefzger,¹⁷⁴ L. Tremblet,³⁰ A. Tricoli,³⁰ I. M. Trigger,^{159a} S. Trincaz-Duvold,⁸⁰
M. F. Tripiana,¹² W. Trischuk,¹⁵⁸ B. Trocmé,⁵⁵ C. Troncon,^{91a} M. Trottier-McDonald,¹⁵ M. Trottelli,¹⁶⁹ P. True,⁹⁰
L. Truong,^{164a,164c} M. Trzebinski,³⁹ A. Trzupek,³⁹ C. Tsarouchas,³⁰ J. C-L. Tseng,¹²⁰ P. V. Tsiareshka,⁹² D. Tsionou,¹⁵⁴

- G. Tsipolitis,¹⁰ N. Tsirintanis,⁹ S. Tsiskaridze,¹² V. Tsiskaridze,⁴⁸ E. G. Tskhadadze,^{51a} I. I. Tsukerman,⁹⁷ V. Tsulaia,¹⁵ S. Tsuno,⁶⁶ D. Tsybychev,¹⁴⁸ A. Tudorache,^{26a} V. Tudorache,^{26a} A. N. Tuna,¹²² S. A. Tupputi,^{20a,20b} S. Turchikhin,^{99,af} D. Turecek,¹²⁸ R. Turra,^{91a,91b} A. J. Turvey,⁴⁰ P. M. Tuts,³⁵ A. Tykhanov,⁴⁹ M. Tylmad,^{146a,146b} M. Tyndel,¹³¹ I. Ueda,¹⁵⁵ R. Ueno,²⁹ M. Ughetto,^{146a,146b} M. Uhlenbrock,²¹ F. Ukegawa,¹⁶⁰ G. Unal,³⁰ A. Undrus,²⁵ G. Unel,¹⁶³ F. C. Ungaro,⁴⁸ Y. Unno,⁶⁶ C. Unverdorben,¹⁰⁰ J. Urban,^{144b} P. Urquijo,⁸⁸ P. Urrejola,⁸³ G. Usai,⁸ A. Usanova,⁶² L. Vacavant,⁸⁵ V. Vacek,¹²⁸ B. Vachon,⁸⁷ C. Valderanis,⁸³ N. Valencic,¹⁰⁷ S. Valentinetti,^{20a,20b} A. Valero,¹⁶⁷ L. Valery,¹² S. Valkar,¹²⁹ E. Valladolid Gallego,¹⁶⁷ S. Vallecorsa,⁴⁹ J. A. Valls Ferrer,¹⁶⁷ W. Van Den Wollenberg,¹⁰⁷ P. C. Van Der Deijl,¹⁰⁷ R. van der Geer,¹⁰⁷ H. van der Graaf,¹⁰⁷ R. Van Der Leeuw,¹⁰⁷ N. van Eldik,¹⁵² P. van Gemmeren,⁶ J. Van Nieuwkoop,¹⁴² I. van Vulpen,¹⁰⁷ M. C. van Woerden,³⁰ M. Vanadia,^{132a,132b} W. Vandelli,³⁰ R. Vanguri,¹²² A. Vaniachine,⁶ F. Vannucci,⁸⁰ G. Vardanyan,¹⁷⁷ R. Vari,^{132a} E. W. Varnes,⁷ T. Varol,⁴⁰ D. Varouchas,⁸⁰ A. Vartapetian,⁸ K. E. Varvell,¹⁵⁰ F. Vazeille,³⁴ T. Vazquez Schroeder,⁸⁷ J. Veatch,⁷ L. M. Veloce,¹⁵⁸ F. Veloso,^{126a,126c} T. Velz,²¹ S. Veneziano,^{132a} A. Ventura,^{73a,73b} D. Ventura,⁸⁶ M. Venturi,¹⁶⁹ N. Venturi,¹⁵⁸ A. Venturini,²³ V. Vercesi,^{121a} M. Verducci,^{132a,132b} W. Verkerke,¹⁰⁷ J. C. Vermeulen,¹⁰⁷ A. Vest,⁴⁴ M. C. Vetterli,^{142,d} O. Viazlo,⁸¹ I. Vichou,¹⁶⁵ T. Vickey,¹³⁹ O. E. Vickey Boeriu,¹³⁹ G. H. A. Viehhäuser,¹²⁰ S. Viel,¹⁵ R. Vigne,⁶² M. Villa,^{20a,20b} M. Villaplana Perez,^{91a,91b} E. Vilucchi,⁴⁷ M. G. Vincter,²⁹ V. B. Vinogradov,⁶⁵ I. Vivarelli,¹⁴⁹ F. Vives Vaque,³ S. Vlachos,¹⁰ D. Vladoiu,¹⁰⁰ M. Vlasak,¹²⁸ M. Vogel,^{32a} P. Vokac,¹²⁸ G. Volpi,^{124a,124b} M. Volpi,⁸⁸ H. von der Schmitt,¹⁰¹ H. von Radziewski,⁴⁸ E. von Toerne,²¹ V. Vorobel,¹²⁹ K. Vorobev,⁹⁸ M. Vos,¹⁶⁷ R. Voss,³⁰ J. H. Vossebeld,⁷⁴ N. Vranjes,¹³ M. Vranjes Milosavljevic,¹³ V. Vrba,¹²⁷ M. Vreeswijk,¹⁰⁷ R. Vuillermet,³⁰ I. Vukotic,³¹ Z. Vykydal,¹²⁸ P. Wagner,²¹ W. Wagner,¹⁷⁵ H. Wahlberg,⁷¹ S. Wahrmund,⁴⁴ J. Wakabayashi,¹⁰³ J. Walder,⁷² R. Walker,¹⁰⁰ W. Walkowiak,¹⁴¹ C. Wang,¹⁵¹ F. Wang,¹⁷³ H. Wang,¹⁵ H. Wang,⁴⁰ J. Wang,⁴² J. Wang,^{33a} K. Wang,⁸⁷ R. Wang,⁶ S. M. Wang,¹⁵¹ T. Wang,²¹ T. Wang,³⁵ X. Wang,¹⁷⁶ C. Wanotayaroj,¹¹⁶ A. Warburton,⁸⁷ C. P. Ward,²⁸ D. R. Wardrope,⁷⁸ M. Warsinsky,⁴⁸ A. Washbrook,⁴⁶ C. Wasicki,⁴² P. M. Watkins,¹⁸ A. T. Watson,¹⁸ I. J. Watson,¹⁵⁰ M. F. Watson,¹⁸ G. Watts,¹³⁸ S. Watts,⁸⁴ B. M. Waugh,⁷⁸ S. Webb,⁸⁴ M. S. Weber,¹⁷ S. W. Weber,¹⁷⁴ J. S. Webster,³¹ A. R. Weidberg,¹²⁰ B. Weinert,⁶¹ J. Weingarten,⁵⁴ C. Weiser,⁴⁸ H. Weits,¹⁰⁷ P. S. Wells,³⁰ T. Wenaus,²⁵ T. Wengler,³⁰ S. Wenig,³⁰ N. Wermes,²¹ M. Werner,⁴⁸ P. Werner,³⁰ M. Wessels,^{58a} J. Wetter,¹⁶¹ K. Whalen,¹¹⁶ A. M. Wharton,⁷² A. White,⁸ M. J. White,¹ R. White,^{32b} S. White,^{124a,124b} D. Whiteson,¹⁶³ F. J. Wickens,¹³¹ W. Wiedenmann,¹⁷³ M. Wielers,¹³¹ P. Wienemann,²¹ C. Wiglesworth,³⁶ L. A. M. Wiik-Fuchs,²¹ A. Wildauer,¹⁰¹ H. G. Wilkens,³⁰ H. H. Williams,¹²² S. Williams,¹⁰⁷ C. Willis,⁹⁰ S. Willocq,⁸⁶ A. Wilson,⁸⁹ J. A. Wilson,¹⁸ I. Wingerter-Seez,⁵ F. Winkelmeier,¹¹⁶ B. T. Winter,²¹ M. Wittgen,¹⁴³ J. Wittkowski,¹⁰⁰ S. J. Wollstadt,⁸³ M. W. Wolter,³⁹ H. Wolters,^{126a,126c} B. K. Wosiek,³⁹ J. Wotschack,³⁰ M. J. Woudstra,⁸⁴ K. W. Wozniak,³⁹ M. Wu,⁵⁵ M. Wu,³¹ S. L. Wu,¹⁷³ X. Wu,⁴⁹ Y. Wu,⁸⁹ T. R. Wyatt,⁸⁴ B. M. Wynne,⁴⁶ S. Xella,³⁶ D. Xu,^{33a} L. Xu,^{33b,aj} B. Yabsley,¹⁵⁰ S. Yacoob,^{145a} R. Yakabe,⁶⁷ M. Yamada,⁶⁶ Y. Yamaguchi,¹¹⁸ A. Yamamoto,⁶⁶ S. Yamamoto,¹⁵⁵ T. Yamanaka,¹⁵⁵ K. Yamauchi,¹⁰³ Y. Yamazaki,⁶⁷ Z. Yan,²² H. Yang,^{33e} H. Yang,¹⁷³ Y. Yang,¹⁵¹ W.-M. Yao,¹⁵ Y. Yasu,⁶⁶ E. Yatsenko,⁵ K. H. Yau Wong,²¹ J. Ye,⁴⁰ S. Ye,²⁵ I. Yeletskikh,⁶⁵ A. L. Yen,⁵⁷ E. Yildirim,⁴² K. Yorita,¹⁷¹ R. Yoshida,⁶ K. Yoshihara,¹²² C. Young,¹⁴³ C. J. S. Young,³⁰ S. Youssef,²² D. R. Yu,¹⁵ J. Yu,⁸ J. M. Yu,⁸⁹ J. Yu,¹¹⁴ L. Yuan,⁶⁷ S. P. Y. Yuen,²¹ A. Yurkewicz,¹⁰⁸ I. Yusuff,^{28,ak} B. Zabinski,³⁹ R. Zaidan,⁶³ A. M. Zaitsev,^{130,aa} J. Zalieckas,¹⁴ A. Zaman,¹⁴⁸ S. Zambito,⁵⁷ L. Zanello,^{132a,132b} D. Zanzi,⁸⁸ C. Zeitnitz,¹⁷⁵ M. Zeman,¹²⁸ A. Zemla,^{38a} K. Zengel,²³ O. Zenin,¹³⁰ T. Ženiš,^{144a} D. Zerwas,¹¹⁷ D. Zhang,⁸⁹ F. Zhang,¹⁷³ H. Zhang,^{33c} J. Zhang,⁶ L. Zhang,⁴⁸ R. Zhang,^{33b} X. Zhang,^{33d} Z. Zhang,¹¹⁷ X. Zhao,⁴⁰ Y. Zhao,^{33d,117} Z. Zhao,^{33b} A. Zhemchugov,⁶⁵ J. Zhong,¹²⁰ B. Zhou,⁸⁹ C. Zhou,⁴⁵ L. Zhou,³⁵ L. Zhou,⁴⁰ N. Zhou,¹⁶³ C. G. Zhu,^{33d} H. Zhu,^{33a} J. Zhu,⁸⁹ Y. Zhu,^{33b} X. Zhuang,^{33a} K. Zhukov,⁹⁶ A. Zibell,¹⁷⁴ D. Ziemska,⁶¹ N. I. Zimine,⁶⁵ C. Zimmermann,⁸³ S. Zimmermann,⁴⁸ Z. Zinonos,⁵⁴ M. Zinser,⁸³ M. Ziolkowski,¹⁴¹ L. Živković,¹³ G. Zobernig,¹⁷³ A. Zoccoli,^{20a,20b} M. zur Nedden,¹⁶ G. Zurzolo,^{104a,104b} and L. Zwalski³⁰

(ATLAS Collaboration)

¹*Department of Physics, University of Adelaide, Adelaide, Australia*²*Physics Department, SUNY Albany, Albany NY, United States of America*³*Department of Physics, University of Alberta, Edmonton AB, Canada*^{4a}*Department of Physics, Ankara University, Ankara*^{4b}*Istanbul Aydin University, Istanbul*^{4c}*Division of Physics, TOBB University of Economics and Technology, Ankara, Turkey*⁵*LAPP, CNRS/IN2P3 and Université Savoie Mont Blanc, Annecy-le-Vieux, France*⁶*High Energy Physics Division, Argonne National Laboratory, Argonne IL, United States of America*⁷*Department of Physics, University of Arizona, Tucson AZ, United States of America*⁸*Department of Physics, The University of Texas at Arlington, Arlington TX, United States of America*⁹*Physics Department, University of Athens, Athens, Greece*¹⁰*Physics Department, National Technical University of Athens, Zografou, Greece*¹¹*Institute of Physics, Azerbaijan Academy of Sciences, Baku, Azerbaijan*¹²*Institut de Física d'Altes Energies and Departament de Física de la Universitat Autònoma de Barcelona, Barcelona, Spain*¹³*Institute of Physics, University of Belgrade, Belgrade, Serbia*

¹⁴*Department for Physics and Technology, University of Bergen, Bergen, Norway*¹⁵*Physics Division, Lawrence Berkeley National Laboratory and University of California, Berkeley CA, United States of America*¹⁶*Department of Physics, Humboldt University, Berlin, Germany*¹⁷*Albert Einstein Center for Fundamental Physics and Laboratory for High Energy Physics, University of Bern, Bern, Switzerland*¹⁸*School of Physics and Astronomy, University of Birmingham, Birmingham, United Kingdom*^{19a}*Department of Physics, Bogazici University, Istanbul*^{19b}*Department of Physics Engineering, Gaziantep University, Gaziantep*^{19c}*Department of Physics, Dogus University, Istanbul, Turkey*^{20a}*INFN Sezione di Bologna*^{20b}*Dipartimento di Fisica e Astronomia, Università di Bologna, Bologna, Italy*²¹*Physikalisches Institut, University of Bonn, Bonn, Germany*²²*Department of Physics, Boston University, Boston MA, United States of America*²³*Department of Physics, Brandeis University, Waltham MA, United States of America*^{24a}*Universidade Federal do Rio De Janeiro COPPE/EE/IF, Rio de Janeiro*^{24b}*Electrical Circuits Department, Federal University of Juiz de Fora (UFJF), Juiz de Fora*^{24c}*Federal University of Sao Joao del Rei (UFSJ), Sao Joao del Rei*^{24d}*Instituto de Fisica, Universidade de Sao Paulo, Sao Paulo, Brazil*²⁵*Physics Department, Brookhaven National Laboratory, Upton NY, United States of America*^{26a}*National Institute of Physics and Nuclear Engineering, Bucharest*^{26b}*National Institute for Research and Development of Isotopic and Molecular Technologies, Physics Department, Cluj Napoca*^{26c}*University Politehnica Bucharest, Bucharest*^{26d}*West University in Timisoara, Timisoara, Romania*²⁷*Departamento de Física, Universidad de Buenos Aires, Buenos Aires, Argentina*²⁸*Cavendish Laboratory, University of Cambridge, Cambridge, United Kingdom*²⁹*Department of Physics, Carleton University, Ottawa ON, Canada*³⁰*CERN, Geneva, Switzerland*³¹*Enrico Fermi Institute, University of Chicago, Chicago IL, United States of America*^{32a}*Departamento de Física, Pontifícia Universidad Católica de Chile, Santiago*^{32b}*Departamento de Física, Universidad Técnica Federico Santa María, Valparaíso, Chile*^{33a}*Institute of High Energy Physics, Chinese Academy of Sciences, Beijing*^{33b}*Department of Modern Physics, University of Science and Technology of China, Anhui*^{33c}*Department of Physics, Nanjing University, Jiangsu*^{33d}*School of Physics, Shandong University, Shandong*^{33e}*Department of Physics and Astronomy, Shanghai Key Laboratory for Particle Physics and Cosmology,**Shanghai Jiao Tong University, Shanghai*^{33f}*Physics Department, Tsinghua University, Beijing 100084, China*³⁴*Laboratoire de Physique Corpusculaire, Clermont Université and Université Blaise Pascal and CNRS/IN2P3, Clermont-Ferrand, France*³⁵*Nevis Laboratory, Columbia University, Irvington NY, United States of America*³⁶*Niels Bohr Institute, University of Copenhagen, Kobenhavn, Denmark*^{37a}*INFN Gruppo Collegato di Cosenza, Laboratori Nazionali di Frascati*^{37b}*Dipartimento di Fisica, Università della Calabria, Rende, Italy*^{38a}*AGH University of Science and Technology, Faculty of Physics and Applied Computer Science, Krakow*^{38b}*Marian Smoluchowski Institute of Physics, Jagiellonian University, Krakow, Poland*³⁹*Institute of Nuclear Physics Polish Academy of Sciences, Krakow, Poland*⁴⁰*Physics Department, Southern Methodist University, Dallas TX, United States of America*⁴¹*Physics Department, University of Texas at Dallas, Richardson TX, United States of America*⁴²*DESY, Hamburg and Zeuthen, Germany*⁴³*Institut für Experimentelle Physik IV, Technische Universität Dortmund, Dortmund, Germany*⁴⁴*Institut für Kern- und Teilchenphysik, Technische Universität Dresden, Dresden, Germany*⁴⁵*Department of Physics, Duke University, Durham, NC, United States of America*⁴⁶*SUPA - School of Physics and Astronomy, University of Edinburgh, Edinburgh, United Kingdom*⁴⁷*INFN Laboratori Nazionali di Frascati, Frascati, Italy*⁴⁸*Fakultät für Mathematik und Physik, Albert-Ludwigs-Universität, Freiburg, Germany*⁴⁹*Section de Physique, Université de Genève, Geneva, Switzerland*^{50a}*INFN Sezione di Genova*^{50b}*Dipartimento di Fisica, Università di Genova, Genova, Italy*^{51a}*E. Andronikashvili Institute of Physics, Iv. Javakhishvili Tbilisi State University, Tbilisi*^{51b}*High Energy Physics Institute, Tbilisi State University, Tbilisi, Georgia*⁵²*II Physikalisches Institut, Justus-Liebig-Universität Giessen, Giessen, Germany*

- ⁵³SUPA—*School of Physics and Astronomy, University of Glasgow, Glasgow, United Kingdom*
- ⁵⁴*II Physikalisches Institut, Georg-August-Universität, Göttingen, Germany*
- ⁵⁵*Laboratoire de Physique Subatomique et de Cosmologie, Université Grenoble-Alpes, CNRS/IN2P3, Grenoble, France*
- ⁵⁶*Department of Physics, Hampton University, Hampton, VA, United States of America*
- ⁵⁷*Laboratory for Particle Physics and Cosmology, Harvard University, Cambridge, MA, United States of America*
- ^{58a}*Kirchhoff-Institut für Physik, Ruprecht-Karls-Universität Heidelberg, Heidelberg*
- ^{58b}*Physikalisches Institut, Ruprecht-Karls-Universität Heidelberg, Heidelberg*
- ^{58c}*ZITI Institut für technische Informatik, Ruprecht-Karls-Universität Heidelberg, Mannheim, Germany*
- ⁵⁹*Faculty of Applied Information Science, Hiroshima Institute of Technology, Hiroshima, Japan*
- ^{60a}*Department of Physics, The Chinese University of Hong Kong, Shatin, N.T., Hong Kong*
- ^{60b}*Department of Physics, The University of Hong Kong, Hong Kong*
- ^{60c}*Department of Physics, The Hong Kong University of Science and Technology, Clear Water Bay, Kowloon, Hong Kong, China*
- ⁶¹*Department of Physics, Indiana University, Bloomington, IN, United States of America*
- ⁶²*Institut für Astro- und Teilchenphysik, Leopold-Franzens-Universität, Innsbruck, Austria*
- ⁶³*University of Iowa, Iowa City, IA, United States of America*
- ⁶⁴*Department of Physics and Astronomy, Iowa State University, Ames, IA, United States of America*
- ⁶⁵*Joint Institute for Nuclear Research, JINR Dubna, Dubna, Russia*
- ⁶⁶*KEK, High Energy Accelerator Research Organization, Tsukuba, Japan*
- ⁶⁷*Graduate School of Science, Kobe University, Kobe, Japan*
- ⁶⁸*Faculty of Science, Kyoto University, Kyoto, Japan*
- ⁶⁹*Kyoto University of Education, Kyoto, Japan*
- ⁷⁰*Department of Physics, Kyushu University, Fukuoka, Japan*
- ⁷¹*Instituto de Física La Plata, Universidad Nacional de La Plata and CONICET, La Plata, Argentina*
- ⁷²*Physics Department, Lancaster University, Lancaster, United Kingdom*
- ^{73a}*INFN Sezione di Lecce*
- ^{73b}*Dipartimento di Matematica e Fisica, Università del Salento, Lecce, Italy*
- ⁷⁴*Oliver Lodge Laboratory, University of Liverpool, Liverpool, United Kingdom*
- ⁷⁵*Department of Physics, Jožef Stefan Institute and University of Ljubljana, Ljubljana, Slovenia*
- ⁷⁶*School of Physics and Astronomy, Queen Mary University of London, London, United Kingdom*
- ⁷⁷*Department of Physics, Royal Holloway University of London, Surrey, United Kingdom*
- ⁷⁸*Department of Physics and Astronomy, University College London, London, United Kingdom*
- ⁷⁹*Louisiana Tech University, Ruston, LA, United States of America*
- ⁸⁰*Laboratoire de Physique Nucléaire et de Hautes Energies, UPMC and Université Paris-Diderot and CNRS/IN2P3, Paris, France*
- ⁸¹*Fysiska Institutionen, Lunds Universitet, Lund, Sweden*
- ⁸²*Departamento de Física Teórica C-15, Universidad Autónoma de Madrid, Madrid, Spain*
- ⁸³*Institut für Physik, Universität Mainz, Mainz, Germany*
- ⁸⁴*School of Physics and Astronomy, University of Manchester, Manchester, United Kingdom*
- ⁸⁵*CPPM, Aix-Marseille Université and CNRS/IN2P3, Marseille, France*
- ⁸⁶*Department of Physics, University of Massachusetts, Amherst, MA, United States of America*
- ⁸⁷*Department of Physics, McGill University, Montreal, QC, Canada*
- ⁸⁸*School of Physics, University of Melbourne, Melbourne, VIC, Australia*
- ⁸⁹*Department of Physics, The University of Michigan, Ann Arbor, MI, United States of America*
- ⁹⁰*Department of Physics and Astronomy, Michigan State University, East Lansing, MI, United States of America*
- ^{91a}*INFN Sezione di Milano*
- ^{91b}*Dipartimento di Fisica, Università di Milano, Milano, Italy*
- ⁹²*B. I. Stepanov Institute of Physics, National Academy of Sciences of Belarus, Minsk, Republic of Belarus*
- ⁹³*National Scientific and Educational Centre for Particle and High Energy Physics, Minsk, Republic of Belarus*
- ⁹⁴*Department of Physics, Massachusetts Institute of Technology, Cambridge, MA, United States of America*
- ⁹⁵*Group of Particle Physics, University of Montreal, Montreal, QC, Canada*
- ⁹⁶*P. N. Lebedev Institute of Physics, Academy of Sciences, Moscow, Russia*
- ⁹⁷*Institute for Theoretical and Experimental Physics (ITEP), Moscow, Russia*
- ⁹⁸*National Research Nuclear University MEPhI, Moscow, Russia*
- ⁹⁹*D.V. Skobeltsyn Institute of Nuclear Physics, M.V. Lomonosov Moscow State University, Moscow, Russia*
- ¹⁰⁰*Fakultät für Physik, Ludwig-Maximilians-Universität München, München, Germany*
- ¹⁰¹*Max-Planck-Institut für Physik (Werner-Heisenberg-Institut), München, Germany*
- ¹⁰²*Nagasaki Institute of Applied Science, Nagasaki, Japan*
- ¹⁰³*Graduate School of Science and Kobayashi-Maskawa Institute, Nagoya University, Nagoya, Japan*
- ^{104a}*INFN Sezione di Napoli*
- ^{104b}*Dipartimento di Fisica, Università di Napoli, Napoli, Italy*

- ¹⁰⁵Department of Physics and Astronomy, University of New Mexico, Albuquerque, NM, United States of America
¹⁰⁶Institute for Mathematics, Astrophysics and Particle Physics, Radboud University Nijmegen/Nikhef, Nijmegen, The Netherlands
¹⁰⁷Nikhef National Institute for Subatomic Physics and University of Amsterdam, Amsterdam, The Netherlands
¹⁰⁸Department of Physics, Northern Illinois University, DeKalb, IL, United States of America
¹⁰⁹Budker Institute of Nuclear Physics, SB RAS, Novosibirsk, Russia
¹¹⁰Department of Physics, New York University, New York, NY, United States of America
¹¹¹Ohio State University, Columbus, OH, United States of America
¹¹²Faculty of Science, Okayama University, Okayama, Japan
¹¹³Homer L. Dodge Department of Physics and Astronomy, University of Oklahoma, Norman, OK, United States of America
¹¹⁴Department of Physics, Oklahoma State University, Stillwater, OK, United States of America
¹¹⁵Palacký University, RCPMT, Olomouc, Czech Republic
¹¹⁶Center for High Energy Physics, University of Oregon, Eugene, OR, United States of America
¹¹⁷LAL, Université Paris-Sud and CNRS/IN2P3, Orsay, France
¹¹⁸Graduate School of Science, Osaka University, Osaka, Japan
¹¹⁹Department of Physics, University of Oslo, Oslo, Norway
¹²⁰Department of Physics, Oxford University, Oxford, United Kingdom
^{121a}INFN Sezione di Pavia
^{121b}Dipartimento di Fisica, Università di Pavia, Pavia, Italy
¹²²Department of Physics, University of Pennsylvania, Philadelphia, PA, United States of America
¹²³National Research Centre “Kurchatov Institute” B.P. Konstantinov Petersburg Nuclear Physics Institute, St. Petersburg, Russia
^{124a}INFN Sezione di Pisa
^{124b}Dipartimento di Fisica E. Fermi, Università di Pisa, Pisa, Italy
¹²⁵Department of Physics and Astronomy, University of Pittsburgh, Pittsburgh, PA, United States of America
^{126a}Laboratório de Instrumentação e Física Experimental de Partículas—LIP, Lisboa
^{126b}Faculdade de Ciências, Universidade de Lisboa, Lisboa
^{126c}Department of Physics, University of Coimbra, Coimbra
^{126d}Centro de Física Nuclear da Universidade de Lisboa, Lisboa
^{126e}Departamento de Física, Universidade do Minho, Braga
^{126f}Departamento de Física Teórica y del Cosmos and CAFPE, Universidad de Granada, Granada, Spain
^{126g}Departamento de Física and CEFITEC of Faculdade de Ciencias e Tecnologia, Universidade Nova de Lisboa, Caparica, Portugal
¹²⁷Institute of Physics, Academy of Sciences of the Czech Republic, Praha, Czech Republic
¹²⁸Czech Technical University in Prague, Praha, Czech Republic
¹²⁹Faculty of Mathematics and Physics, Charles University in Prague, Praha, Czech Republic
¹³⁰State Research Center Institute for High Energy Physics, Protvino, Russia
¹³¹Particle Physics Department, Rutherford Appleton Laboratory, Didcot, United Kingdom
^{132a}INFN Sezione di Roma
^{132b}Dipartimento di Fisica, Sapienza Università di Roma, Roma, Italy
^{133a}INFN Sezione di Roma Tor Vergata
^{133b}Dipartimento di Fisica, Università di Roma Tor Vergata, Roma, Italy
^{134a}INFN Sezione di Roma Tre
^{134b}Dipartimento di Matematica e Fisica, Università Roma Tre, Roma, Italy
^{135a}Faculté des Sciences Ain Chock, Réseau Universitaire de Physique des Hautes Energies—Université Hassan II, Casablanca
^{135b}Centre National de l’Energie des Sciences Techniques Nucléaires, Rabat
^{135c}Faculté des Sciences Semlalia, Université Cadi Ayyad, LPHEA-Marrakech
^{135d}Faculté des Sciences, Université Mohamed Premier and LPTPM, Oujda
^{135e}Faculté des sciences, Université Mohammed V-Agdal, Rabat, Morocco
¹³⁶DSM/IRFU (Institut de Recherches sur les Lois Fondamentales de l’Univers), CEA Saclay (Commissariat à l’Energie Atomique et aux Energies Alternatives), Gif-sur-Yvette, France
¹³⁷Santa Cruz Institute for Particle Physics, University of California, Santa Cruz, Santa Cruz, CA, United States of America
¹³⁸Department of Physics, University of Washington, Seattle, WA, United States of America
¹³⁹Department of Physics and Astronomy, University of Sheffield, Sheffield, United Kingdom
¹⁴⁰Department of Physics, Shinshu University, Nagano, Japan
¹⁴¹Fachbereich Physik, Universität Siegen, Siegen, Germany
¹⁴²Department of Physics, Simon Fraser University, Burnaby, BC, Canada
¹⁴³SLAC National Accelerator Laboratory, Stanford, CA, United States of America
^{144a}Faculty of Mathematics, Physics & Informatics, Comenius University, Bratislava
^{144b}Department of Subnuclear Physics, Institute of Experimental Physics of the Slovak Academy of Sciences, Kosice, Slovak Republic
^{145a}Department of Physics, University of Cape Town, Cape Town
^{145b}Department of Physics, University of Johannesburg, Johannesburg

- ^{145c}School of Physics, University of the Witwatersrand, Johannesburg, South Africa
^{146a}Department of Physics, Stockholm University
^{146b}The Oskar Klein Centre, Stockholm, Sweden
¹⁴⁷Physics Department, Royal Institute of Technology, Stockholm, Sweden
¹⁴⁸Departments of Physics & Astronomy and Chemistry, Stony Brook University, Stony Brook, NY, United States of America
¹⁴⁹Department of Physics and Astronomy, University of Sussex, Brighton, United Kingdom
¹⁵⁰School of Physics, University of Sydney, Sydney, Australia
¹⁵¹Institute of Physics, Academia Sinica, Taipei, Taiwan
¹⁵²Department of Physics, Technion: Israel Institute of Technology, Haifa, Israel
¹⁵³Raymond and Beverly Sackler School of Physics and Astronomy, Tel Aviv University, Tel Aviv, Israel
¹⁵⁴Department of Physics, Aristotle University of Thessaloniki, Thessaloniki, Greece
¹⁵⁵International Center for Elementary Particle Physics and Department of Physics, The University of Tokyo, Tokyo, Japan
¹⁵⁶Graduate School of Science and Technology, Tokyo Metropolitan University, Tokyo, Japan
¹⁵⁷Department of Physics, Tokyo Institute of Technology, Tokyo, Japan
¹⁵⁸Department of Physics, University of Toronto, Toronto ON, Canada
^{159a}TRIUMF, Vancouver BC
^{159b}Department of Physics and Astronomy, York University, Toronto, ON, Canada
¹⁶⁰Faculty of Pure and Applied Sciences, University of Tsukuba, Tsukuba, Japan
¹⁶¹Department of Physics and Astronomy, Tufts University, Medford, MA, United States of America
¹⁶²Centro de Investigaciones, Universidad Antonio Narino, Bogota, Colombia
¹⁶³Department of Physics and Astronomy, University of California, Irvine, Irvine, CA, United States of America
^{164a}INFN Gruppo Collegato di Udine, Sezione di Trieste, Udine
^{164b}ICTP, Trieste
^{164c}Dipartimento di Chimica, Fisica e Ambiente, Università di Udine, Udine, Italy
¹⁶⁵Department of Physics, University of Illinois, Urbana, IL, United States of America
¹⁶⁶Department of Physics and Astronomy, University of Uppsala, Uppsala, Sweden
¹⁶⁷Instituto de Física Corpuscular (IFIC) and Departamento de Física Atómica, Molecular y Nuclear and Departamento de Ingeniería Electrónica and Instituto de Microelectrónica de Barcelona (IMB-CNM), University of Valencia and CSIC, Valencia, Spain
¹⁶⁸Department of Physics, University of British Columbia, Vancouver, BC, Canada
¹⁶⁹Department of Physics and Astronomy, University of Victoria, Victoria, BC, Canada
¹⁷⁰Department of Physics, University of Warwick, Coventry, United Kingdom
¹⁷¹Waseda University, Tokyo, Japan
¹⁷²Department of Particle Physics, The Weizmann Institute of Science, Rehovot, Israel
¹⁷³Department of Physics, University of Wisconsin, Madison, WI, United States of America
¹⁷⁴Fakultät für Physik und Astronomie, Julius-Maximilians-Universität, Würzburg, Germany
¹⁷⁵Fachbereich C Physik, Bergische Universität Wuppertal, Wuppertal, Germany
¹⁷⁶Department of Physics, Yale University, New Haven, CT, United States of America
¹⁷⁷Yerevan Physics Institute, Yerevan, Armenia
¹⁷⁸Centre de Calcul de l'Institut National de Physique Nucléaire et de Physique des Particules (IN2P3), Villeurbanne, France

^aAlso at Department of Physics, King's College London, London, United Kingdom^bAlso at Institute of Physics, Azerbaijan Academy of Sciences, Baku, Azerbaijan^cAlso at Novosibirsk State University, Novosibirsk, Russia^dAlso at TRIUMF, Vancouver, BC, Canada^eAlso at Department of Physics, California State University, Fresno CA, United States of America^fAlso at Department of Physics, University of Fribourg, Fribourg, Switzerland^gAlso at Departamento de Física e Astronomia, Faculdade de Ciencias, Universidade do Porto, Portugal^hAlso at Tomsk State University, Tomsk, RussiaⁱAlso at CPPM, Aix-Marseille Université and CNRS/IN2P3, Marseille, France^jAlso at Universita di Napoli Parthenope, Napoli, Italy^kAlso at Institute of Particle Physics (IPP), Canada^lAlso at Particle Physics Department, Rutherford Appleton Laboratory, Didcot, United Kingdom^mAlso at Department of Physics, St. Petersburg State Polytechnical University, St. Petersburg, RussiaⁿAlso at Louisiana Tech University, Ruston, LA, United States of America^oAlso at Institutio Catalana de Recerca i Estudis Avancats, ICREA, Barcelona, Spain^pAlso at Department of Physics, National Tsing Hua University, Taiwan^qAlso at Department of Physics, The University of Texas at Austin, Austin, TX, United States of America^rAlso at Institute of Theoretical Physics, Ilia State University, Tbilisi, Georgia^sAlso at CERN, Geneva, Switzerland

^tAlso at Georgian Technical University (GTU), Tbilisi, Georgia^uAlso at Manhattan College, New York, NY, United States of America^vAlso at Hellenic Open University, Patras, Greece^wAlso at Institute of Physics, Academia Sinica, Taipei, Taiwan^xAlso at LAL, Université Paris-Sud and CNRS/IN2P3, Orsay, France^yAlso at Academia Sinica Grid Computing, Institute of Physics, Academia Sinica, Taipei, Taiwan^zAlso at School of Physics, Shandong University, Shandong, China^{aa}Also at Moscow Institute of Physics and Technology State University, Dolgoprudny, Russia^{ab}Also at Section de Physique, Université de Genève, Geneva, Switzerland^{ac}Also at International School for Advanced Studies (SISSA), Trieste, Italy^{ad}Also at Department of Physics and Astronomy, University of South Carolina, Columbia, SC, United States of America^{ae}Also at School of Physics and Engineering, Sun Yat-sen University, Guangzhou, China^{af}Also at Faculty of Physics, M.V. Lomonosov Moscow State University, Moscow, Russia^{ag}Also at National Research Nuclear University MEPhI, Moscow, Russia^{ah}Also at Department of Physics, Stanford University, Stanford, CA, United States of America^{ai}Also at Institute for Particle and Nuclear Physics, Wigner Research Centre for Physics, Budapest, Hungary^{aj}Also at Department of Physics, The University of Michigan, Ann Arbor, MI, United States of America^{ak}Also at University of Malaya, Department of Physics, Kuala Lumpur, Malaysia^{*}Deceased



School of Natural Sciences and Mathematics

*Z Boson Production in $p + Pb$ Collisions at $\sqrt{s}(NN) = 5.02 \text{ TeV}$
Measured with the ATLAS Detector*

CC BY 3.0 (Attribution) License
©2015 CERN, for the ATLAS Collaboration

Citation:

Aad, G., B. Abbott, J. Abdallah, O. Abdinov, et al. 2015. "Z boson production in p plus Pb collisions at root S-NN=5.02 TeV measured with the ATLAS detector." Physical Review C 92(4), doi:10.1103/PhysRevC.92.044915

This document is being made freely available by the Eugene McDermott Library of The University of Texas at Dallas with permission from the copyright owner. All rights are reserved under United States copyright law unless specified otherwise.